



Cite this: *Nanoscale*, 2024, **16**, 10500

## Advanced micro/nano-electroporation for gene therapy: recent advances and future outlook

Feng Liu,<sup>†a</sup> Rongtai Su,<sup>†a</sup> Xinran Jiang,<sup>†a</sup> Siqi Wang,<sup>ID †b</sup> Wei Mu<sup>\*a,c,d</sup> and Lingqian Chang <sup>ID \*a</sup>

Gene therapy is a promising disease treatment approach by editing target genes, and thus plays a fundamental role in precision medicine. To ensure gene therapy efficacy, the effective delivery of therapeutic genes into specific cells is a key challenge. Electroporation utilizes short electric pulses to physically break the cell membrane barrier, allowing gene transfer into the cells. It dodges the off-target risks associated with viral vectors, and also stands out from other physical-based gene delivery methods with its high-throughput and cargo-accelerating features. In recent years, with the help of advanced micro/nano-technology, micro/nanostructure-integrated electroporation (micro/nano-electroporation) techniques and devices have significantly improved cell viability, transfection efficiency and dose controllability of the electroporation strategy, enhancing its application practicality especially *in vivo*. This technical advancement makes micro/nano-electroporation an effective and versatile tool for gene therapy. In this review, we first introduce the evolution of electroporation technique with a brief explanation of the perforation mechanism, and then provide an overview of the recent advancements and prospects of micro/nano-electroporation technology in the field of gene therapy. To comprehensively showcase the latest developments of micro/nano-electroporation technology in gene therapy, we focus on discussing micro/nano-electroporation devices and current applications at both *in vitro* and *in vivo* levels. Additionally, we outline the ongoing clinical studies of gene electrotransfer (GET), revealing the tremendous potential of electroporation-based gene delivery in disease treatment and healthcare. Lastly, the challenges and future directions in this field are discussed.

Received 31st March 2024,  
Accepted 13th May 2024

DOI: 10.1039/d4nr01408a  
[rsc.li/nanoscale](http://rsc.li/nanoscale)

### 1. Introduction

Gene therapy, as a highly promising emerging therapeutic approach, combines the applications of modern molecular biology techniques and precision medical engineering.<sup>1,2</sup> Its earliest concept involves the introduction of DNA fragments containing normal gene sequences into cells to correct gene sequences at mutation sites or insert normal gene sequences at gene deletion sites, ultimately achieving the goal of treating genetic disorders.<sup>3</sup> Since the 1970s, gene therapy techniques have steadily advanced, particularly in the development of viral

and non-viral vectors, leading to the rapid progression of numerous gene therapy strategies into clinical phases.<sup>4,5</sup>

Compared to viral vectors, non-viral vectors such as lipid nanoparticles<sup>6</sup> and extracellular vehicles (EVs)<sup>7</sup> have advantages in terms of simplicity, ease of large-scale production, and low specific immune reactions. However, these conventional non-viral vectors face challenges in delivery efficiency, resulting in lower transient expression of transgenes.<sup>8,9</sup> Therefore, researchers in the field of gene therapy tend to prefer the use of physically-based techniques that are simple and efficient for gene delivery,<sup>10</sup> such as electroporation,<sup>11</sup> microinjection,<sup>12</sup> gene gun,<sup>13</sup> sonoporation,<sup>14</sup> etc. These methods utilize physical means to open the cellular membrane barrier and facilitate successful delivery of genetic material into cells. Among various gene delivery methods, electroporation has gained attention due to its effectiveness in delivering genes with precision and efficiency.<sup>15–17</sup>

Electroporation technology plays a crucial role in gene therapy by temporarily permeabilizing the cell membrane through the application of short electric pulses, opening paths for the entry of therapeutic genes.<sup>17,18</sup> By applying an external electric field, electroporation significantly enhances the

<sup>a</sup>Beijing Advanced Innovation Center for Biomedical Engineering,  
School of Biological Science and Medical Engineering, Beihang University, Beijing,  
100191, China

<sup>b</sup>Department of General Surgery and Obesity and Metabolic Disease Center,  
China-Japan Friendship Hospital, Beijing, 100029, China

<sup>c</sup>School of Engineering Medicine, Beihang University, Beijing, 100191, China

<sup>d</sup>Key Laboratory of Big Data-Based Precision Medicine (Beihang University),  
Ministry of Industry and Information Technology of the People's Republic of China,  
Beijing, 100191, China

†These authors contributed equally to this work.

efficiency of gene delivery into cells, enabling precise treatment of specific cell types or tissues.<sup>19,20</sup> Furthermore, by selecting appropriate electric pulse parameters, the accuracy and efficiency of gene delivery can be ensured while minimizing damage to the cells, providing a more reliable and effective means for gene therapy.<sup>11,18,21</sup>

In recent years, the rapid advancement of nanotechnology and micro/nano fabrication techniques has provided significant impetus for the innovation of electroporation technology. Researchers have achieved remarkable improvements in cell safety and delivery efficiency by finely tuning the parameters of electric pulses and developing highly biocompatible nanoplatforms.<sup>20,22,23</sup> It is worth mentioning that the application scope of electroporation technology has expanded from its initial success in *in vitro* cell studies to targeted therapy *in vivo*, demonstrating its wide potential and immense value in the field of gene therapy.<sup>17,24–26</sup>

In this review, we delve into the latest research achievements and prospects of micro/nano-electroporation technology in the field of gene therapy. Firstly, we provide a concise overview of the working principles and classifications of micro/nano-electroporation technology, laying the foundation for subsequent analysis and discussions. To comprehensively showcase the recent advancements of micro/nano-electroporation technology in the field of gene therapy, we extensively present the devices and practical applications of micro/nano-electroporation techniques at both the *in vitro* and *in vivo* levels. These examples not only demonstrate the technological advancement and practicality but also provide valuable references for future research endeavors. In addition, we have comprehensively reviewed the preclinical research status of micro/nano-electroporation technology, revealing its tremendous potential in disease treatment. Furthermore, we have acknowledged the challenges currently faced in this field and conducted in-depth analysis and prospects for future development. This review aims to assist biomedical researchers in gaining a comprehensive understanding of the latest advancements and prospects of micro/nano-electroporation technology, thereby better exploring, and harnessing the potential of this technique. We anticipate that micro/nano-electroporation technology will play a greater role in the field of gene therapy, providing new ideas and strategies for disease treatment.

## 2. Overview of micro/nano-electroporation

### 2.1. Working principle

Electroporation, also known as electropermeabilization or electrotransfection, involves the application of high-intensity electric fields to cells, resulting in the formation of transient small pores in the cell membrane, thereby significantly enhancing its permeability.<sup>27–29</sup> This phenomenon enables the successful transfer of charged molecules that are typically unable to pass through the cell membrane under normal conditions, such as

nucleic acids,<sup>10,30,31</sup> proteins,<sup>32,33</sup> carbohydrates,<sup>34,35</sup> and dyes,<sup>36–38</sup> into the cells.

Mechanistically, when an external electric field is applied to a cell (Fig. 1a), it causes differential potential changes on the two sides of the cell membrane, resulting in an induced membrane potential difference.<sup>39</sup> When the intensity of the applied electric field is high enough, causing the induced membrane potential to counteract the resting membrane potential, the normal structure of the phospholipid bilayer is temporarily disrupted, forming hydrophilic pores in the cell membrane. This critical level of transmembrane potential is considered the threshold voltage for electroporation, which is typically 0.2–1 V depending on the cell types.<sup>40–42</sup> Once the membrane phospholipids rearrange, exogenous macromolecules (e.g., plasmids) can then enter the cell through these open channels under the electrophoretic acceleration enabled by the electric field. This cargo-accelerating feature, in addition to membrane perforation, allows electroporation to further stand out from other gene delivery methods.<sup>39,43,44</sup>

### 2.2. Technical evolution in electroporation

In recent years, with the assistance of nanotechnology and micro/nano fabrication techniques, electroporation technology has made significant advancements. From the improvement of bulk electroporation (BEP) to microscale electroporation (MEP) and the emergence of nanoscale electroporation (NEP), these developments have addressed the limitations of traditional electroporation systems and achieved advantages such as safe voltage, high cell viability, dose control and application versatility.

**2.2.1. Bulk electroporation (BEP).** BEP is a widely used and cost-effective technique that allows for the simultaneous electroporation of many cells within a relatively short period of time.<sup>20,24,45</sup> In typical BEP procedures, cargos to be delivered are mixed in single cell suspension and loaded into a chamber equipped with electrodes. Subsequently, a pulsed electric field (typically with a strength of  $>600 \text{ V cm}^{-1}$ ) is applied, inducing cell membrane electroporation and intracellular delivery of cargos (Fig. 1b).<sup>10,18,46</sup>

BEP finds extensive applications in gene transfection, cell engineering, and other fields,<sup>47,48</sup> providing a rapid and efficient approach for high-throughput cell processing. However, despite the various advantages of the BEP technique, significant limitations remain. The high voltages required by BEP systems present the most prominent issues. The heat generated and the pH changes caused by high voltages can lead to decreased cell viability. More importantly, high voltage poses significant hurdles in the *in vivo* study and translational development of BEP techniques. Furthermore, in a BEP system, electric field is applied over an environment that is magnitudes larger than cellular dimensions (and hence the name “bulk”), resulting in non-uniform electric field distribution at the individual cell level.<sup>24,49–53</sup> With the assistance of micro/nanostructures, decreasing the scale of the environment over which the electric field is applied could be an effective solution to the above limitations.

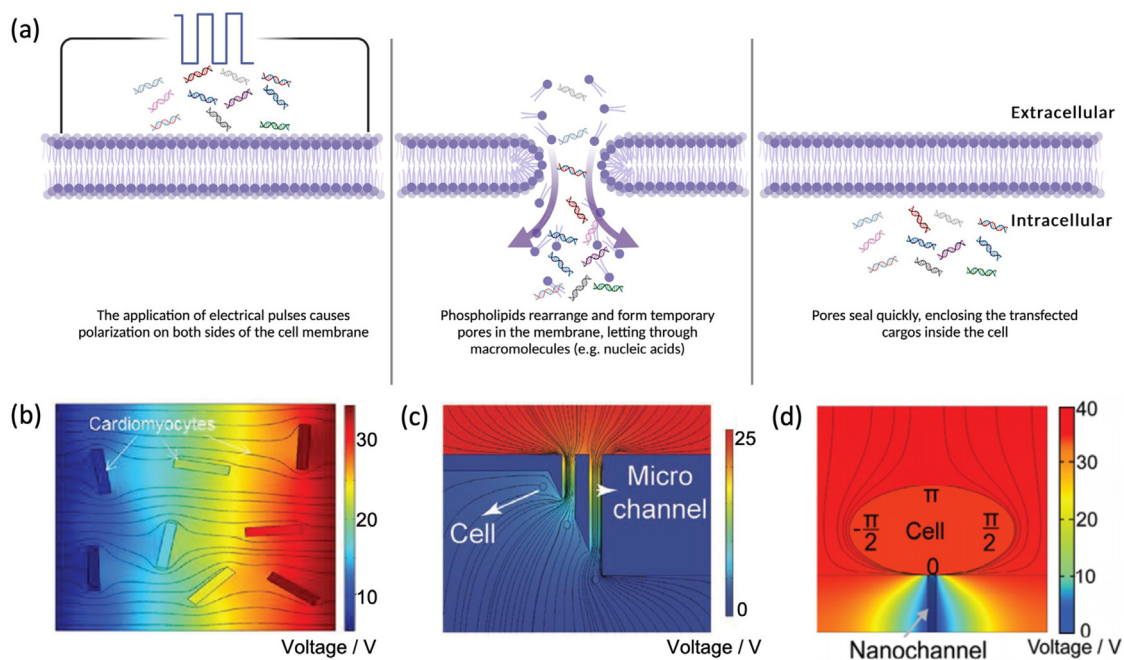


**Fig. 1** Illustration of the mechanism and different configurations of electroporation. (a) Mechanistic illustration of the process of cell electroporation. (b-d) 2D simulation of electric field distribution across the microenvironment of bulk electroporation (BEP) (b),<sup>10</sup> micro-electroporation (MEP) (c),<sup>57</sup> and nano-electroporation (NEP) (d).<sup>59</sup> Reprinted with permission from ref. 10, © 2016 Elsevier; ref. 57, © 2022 Elsevier; ref. 59, © 2024 Elsevier. Created with BioRender.com.

**2.2.2. Micro-electroporation (MEP).** MEP is a technique that utilizes microstructure to achieve cell membrane electroporation for the introduction of exogenous substances into cells.<sup>50,54,55</sup> Compared to traditional BEP techniques, MEP employs micro-electro-mechanical system (MEMS)-fabricated or high-precision 3D printed microscale structures such as microelectrodes and microchannels to apply electric field in a microenvironment (Fig. 1c).<sup>56,57</sup> These structures typically range from a few micrometers to a few hundred micrometers, providing electric field with dimensions comparable to the cell diameters. These localized electric fields act on cells in a more precise and directional manner, inducing electroporation only in specific regions of the target cells, thus enabling more efficient substance delivery than BEP does.<sup>46,50,54,58</sup>

**2.2.3. Nano-electroporation (NEP).** NEP is a novel cell transfection technique that utilizes nanochannels (nanopores) typically ranging from tens to a few hundred of nanometers in diameter to concentrate electric field and perforate cell membrane at highly focalized points (Fig. 1d).<sup>59</sup> Techniques involved in fabricating the required nanostructures include deep reactive ion etching (DRIE) for drilling nanochannels through silicon wafers, and track etching and femtosecond laser for creating nanopores in polymeric membranes.<sup>60,61</sup> The external electric field is concentrated through the nanostructures and exerted on a pinpoint in the cell membrane which is two magnitudes smaller in size than cellular diameters. The finely controlled electrostimulation maximally preserves cell membrane stability at locations other than the

perforation, thus ensuring high cell viability. On the other hand, due to their usually microscale length, the nanochannels act as effective electrical resistances, causing drastic voltage drop of the applied electric field. The voltage drop effect of the commercial nanopore membranes typically reduces electric field strength that is in the lower tens of volts down to  $\sim 1$  V, meeting the requirement of the threshold transmembrane potential for cell membrane disruption. This feature not only endows the applied electric field with controllability and safety, but also significantly enhances the electrophoretic effect on charged molecules within the nanochannels, enabling rapid intracellular transport of desired cargos within microseconds.<sup>62,63</sup> Therefore, compared to BEP and MEP, NEP is able to deliver more molecules before the cell membrane reseals and hence shows further advancement in transfection efficiency.<sup>64</sup>

In summary, the smaller the space to which an external electric field is applied, the lower the strength of the electric field is required for membrane perforation. This is how finer electrode dimensions and nanostructure configurations realized by advanced nanotechnology and micro/nano fabrication techniques help improve cell viability, controllability and safety of electroporation methods. Therefore, NEP represents the latest generation of electroporation approach, with advantages including high safety, high precision, high efficiency, and ease of control over the electrical parameters. With ongoing technical advancements, the potential of NEP technology in biomedical research and applications will continue to be explored and utilized.

### 3. Micro/nano-electroporation system design

The technical evolution from BEP to MEP and NEP entails that finer structure through which the electric field is manipulated gives higher controllability over the electroporation process. This not only enables the improvement of cell viability post-electroporation in general, but also provides a more precise tool for studying the optimal electrical parameters to ensure high transfection efficiency in various types of cells and tissues. As a result, a variety of devices equipped with micro/nanostructures have emerged over the past decade for the *in vitro* or *in vivo* study of electroporation-based gene delivery.<sup>27–29</sup> This section summarizes a few representatives of these micro/nano-electroporation devices.

#### 3.1. *In vitro* electroporation

Electroporation emerged as an *in vitro* intracellular delivery approach for macromolecules such as nucleic acids; with the

technical evolution, the adaptation of micro/nano-electroporation devices for high throughput cell processing *in vitro* still remains the major branch of electroporation application. The devices aimed at serving *in vitro* studies are typically silicon-based platforms equipped with arrays of nanostructures for processing single cells. The *in vitro* environment allows for high levels of freedom in system design, and thus the devices presented below possess a wide range of nanostructures including nanometer-gapped electrode pairs, nanotubes protruding from the chip platform, and commercial track-etched nanopore membrane.<sup>23,56,65</sup> With these nanoscale structures to precisely manipulate how electric field is exerted on cells, researchers are able to improve cell viability, delivery efficiency and dosage controllability substantially.<sup>66–68</sup> These advancements demonstrate the potential applications of this technology in biomedical research and clinical treatment.

Santra *et al.*<sup>23</sup> have designed a nano-localized single-cell nano-electroporation (NL-SCNEP) platform equipped with an array of indium tin oxide (ITO) nanoelectrode pairs (Fig. 2a). Each pair of triangular tipped nanoelectrodes was fabricated

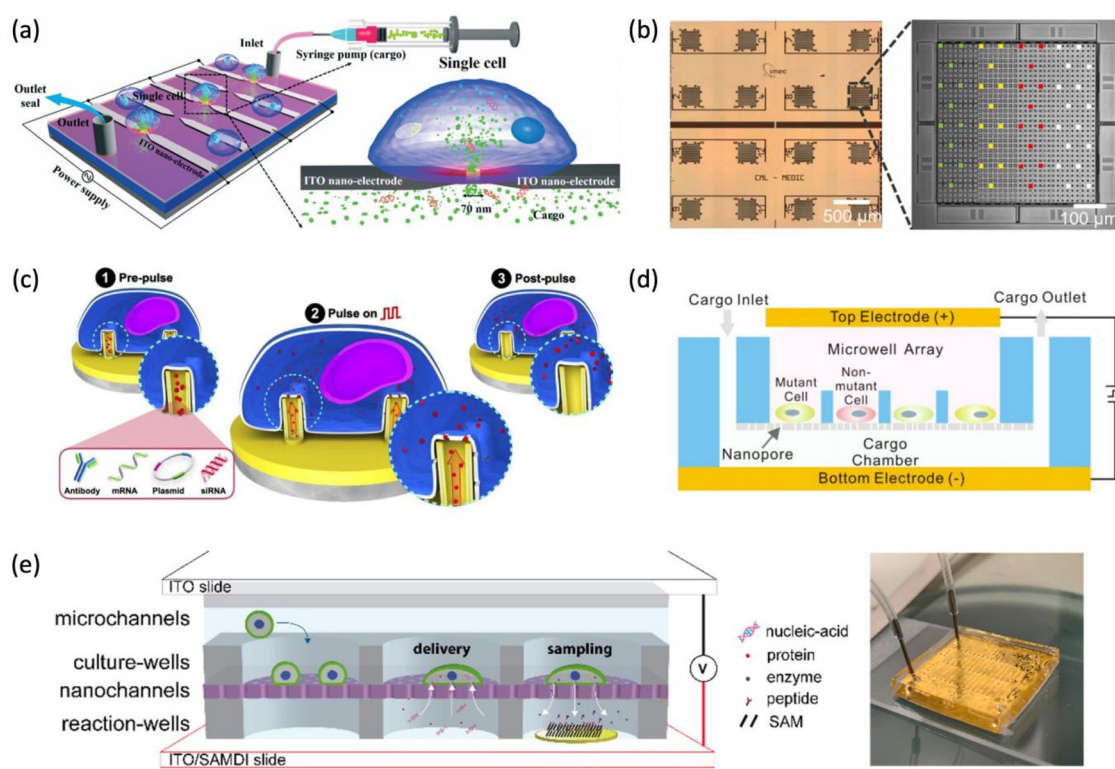


**Fig. 2** Micro/nano-electroporation system for *in vitro* gene therapy. (a) Schematic diagram of the nano-localized single-cell nano-electroporation (NL-SCNEP) chip.<sup>23</sup> (b) Serially enlarged micrographs of the high-definition-electroporation (HD-EP) chip. The microelectrode arrays arranged in 16 clusters were fabricated with complementary metal oxide semiconductor (CMOS) technology (left). Each cluster contains 1024 individually addressable titanium nitride microelectrodes that are sectioned to enable the implementation of 32 different electroporation conditions (right; the four sections marked with different colors represent different electrode sizes, which is one of the five variant parameters).<sup>56</sup> (c) Schematic diagrams of the working electroactive nanoinjection (ENI) platform. Upon the application of external electric pulses, the Au-coated nanotubes cause the formation of localized nanopores in the cell membrane, allowing desired cargos pre-loaded in the nanotubes to transfer intracellularly.<sup>69</sup> (d) A schematic cross-sectional view of the single living cell analysis (SLCA) nanoplateform housing one cell per well.<sup>65</sup> (e) Schematic diagram and photograph of the multi-functioning live-cell analysis device (LCAD).<sup>70</sup> Reprinted with permission from ref. 23 © 2020 the Royal Society of Chemistry; ref. 56 © 2022 Elsevier; ref. 69, © 2023 Nature; ref. 65, © 2021 American Chemical Society; ref. 70 © 2022 American Chemical Society.

by etching an “X” through a single ITO line with the focused ion beam (FIB) technique. The nanoelectrodes each has a tip diameter of 40 nm and the gap between the tips is 70 nm. When a 6 V external electric field is applied through the nano-gap onto the cell membrane, the induced transmembrane potential reaches as high as 2.4 V, sufficiently surpassing the threshold voltage for electroporation. The ITO lines are 10  $\mu\text{m}$  apart, and thus the single cells seeded on the platform may be electroporated at one or multiple sites. With this precise system, Santra and colleagues were able to analyze the temporal and spatial dosage accumulation in single cells by second post delivery, and thereby precisely examine the delivery effects resulting from different electric pulse parameters. From their systematic experimental results, the authors not only concluded that higher voltage and longer pulse duration could result in more/larger pores in the membrane and hence faster intracellular delivery, but also determined the optimal electrical parameters for 4 different types of cells. Specifically, for CL1-0 cells, the NL-SCNEP platform achieved 96% transfection efficiency while maintaining 98% cell viability with the application of a 6 V, 20 ms single pulse.

Duckert *et al.*<sup>56</sup> fully leveraged the multiplexing capability of a multiple-microelectrodes array (MEA) chip for high-definition-electroporation (HD-EP) (Fig. 2b). The subcellular-sized (ranging from 8.75 to 121  $\mu\text{m}^2$ ) microelectrodes are fabricated with complementary metal oxide semi-conductor technology and over 4000 of them are densely arrayed into 16 clusters ( $\sim 0.23 \text{ mm}^2$  each) on a single HD-EP chip. Most importantly, the microelectrodes are individually addressable, allowing them to be used in parallel to screen up to 32 different electroporation conditions simultaneously for the optimal electrical parameters for hard-to-transfect cells such as sensitive primary fibroblasts. The relationships between electroporation parameters and intracellular delivery efficiency or cell survival rate were then modeled by multiple linear regression using quantitative delivery results from experimental conditions with 100 mV- and 100  $\mu\text{s}$ -level differences. The best fitting model for predicting delivery efficiency confirmed the major contributing roles of pulse amplitude and duration among the five variant parameters examined by the authors, which both showed positive linear effect on delivery efficiency. Among the other three parameters, pulse number showed a subtle enhancing effect on delivery efficiency; electrode size presented a negative quadratic effect with the optimal size being 80  $\mu\text{m}^2$  under the chip setting, and pulse symmetry demonstrated better than asymmetry. However, the model for predicting cell survival rate presented contrary trends: both pulse amplitude and electrode size showed negative effect on post-delivery cell viability, and symmetric pulses showed more cytotoxicity than asymmetric ones. These opposing trends by the two models imply an inevitable compromise between cell viability and delivery efficiency when selecting electroporation parameters. Based on these models, Duckert and colleagues were able to apply the optimal electroporation parameters on primary human fibroblasts and achieved  $>81\%$  mRNA transfection efficiency while maintaining 93% cell survival rate. This  $\sim 75\%$

transfection yield (transfection efficiency  $\times$  cell survival rate) makes HD-EP one of the most efficient single-cell transfection technologies with significantly better performance than commercial electroporators on primary cells. This system allows researchers to quickly screen out the optimal electroporation parameters for different types of cells and molecules in a high-throughput manner, which bears immense potential in drug screening and genetic studies, providing new technical support for the development of these fields.

Shokouhi *et al.*<sup>69</sup> proposed an innovative non-viral, low-pressure, and reusable electroactive nanoinjection (EIN) platform based on vertically aligned conductive nanotubes design (Fig. 2c). This platform demonstrated its remarkable capability for localized and efficient delivery of various substances including antibodies, mRNA, and plasmid DNA into mouse fibroblast cells while maintaining over 90% cell viability post-delivery.

Our team<sup>65</sup> has developed a novel high-throughput single living cell analysis (SLCA) platform utilizing NEP technology (Fig. 2d). The core advantage of this platform lies in its ability to efficiently electro-deliver multiple Domino-probes (reporter DNA probes that give off fluorescent signals in the presence of target RNA) into single cells, enabling the precise detection of gene mutations at single-cell level. The SLCA platform also incorporates a vacuum-based advanced device specifically designed to efficiently load cells into the microwells, which reached  $>85\%$  loading efficiency for three different cell lines. Moreover, the SLCA platform achieves delivery efficiency and cell viability both exceeding 90%, indicating its suitability for analyzing genetic mutations and drug resistance in living cells.

Patino *et al.*<sup>70</sup> reported a multimodal live-cell analysis device (LCAD), in a microarray format that utilizes localized electroporation to achieve reversible perforation of cell membranes for the delivery of exogenous substances or the sampling of intracellular contents (Fig. 2e). Meanwhile the platform's localized electroporation mechanism is non-destructive and enables multiple stimulation and time-dependent molecular sampling of living cells, providing new possibilities for the study of dynamic cellular processes. The emergence of this groundbreaking platform not only provides powerful technical support for live cell analysis but also significantly enhances the accuracy and efficiency of the analysis.

In summary, micro/nano-electroporation devices hold a significant position in the field of *ex vivo* gene therapy. They not only greatly enhanced the efficiency and precision of gene therapy, but also drove innovation and development in related technologies. Moreover, they play a crucial role in improving treatment safety and controllability. Therefore, research and application of micro/nano-electroporation devices have profound significance for the advancement of the field of gene therapy.

### 3.2. *In vivo* electroporation

Traditional gene therapy often involves manipulating cells *ex vivo* and then reintroducing the modified cells back into the

body. However, this method needs to be improved in terms of operational procedures and immune rejection, which makes more and more researchers tend to choose the method of direct *in vivo* gene therapy, in order to obtain more direct and efficient treatment effects.<sup>1,3,71</sup> *In vivo* micro/nano-electroporation devices allow for direct gene manipulation of cells within the body, avoiding the cumbersome process of *ex vivo* cultivation and significantly improving treatment efficiency. Furthermore, by performing the manipulation directly *in vivo*, the devices reduce the potential for cell mutations and contamination that may occur during *ex vivo* cultivation, thereby enhancing the safety of the treatment.<sup>72</sup> Kougkulos *et al.*<sup>73</sup> creatively invented a conductive nanocomposite hydrogel. This hydrogel incorporates conductive carbon nanotubes into a highly hydrophilic and biocompatible agarose polymer matrix,

serving not only as a drug reservoir but also as an electrode for applying electric pulses to the skin (Fig. 3a). They comprehensively evaluated the effects of skin electroporation and drug delivery using a multi-scale approach. During the electroporation process, they performed real-time electrical measurements, conducted systematic numerical simulations, and validated them with fluorescent molecule transfer. Firstly, they applied pulse electric fields and precisely measured changes in skin resistance before, during, and after pulse application. Subsequently, they used this data to fine-tune the numerical model of the system. Finally, they compared the model with transdermal delivery of fluorescent molecules. By utilizing fluorescent moieties with different properties, they successfully identified the threshold for disrupting the skin barrier function (300 V). This series of operations not only improved

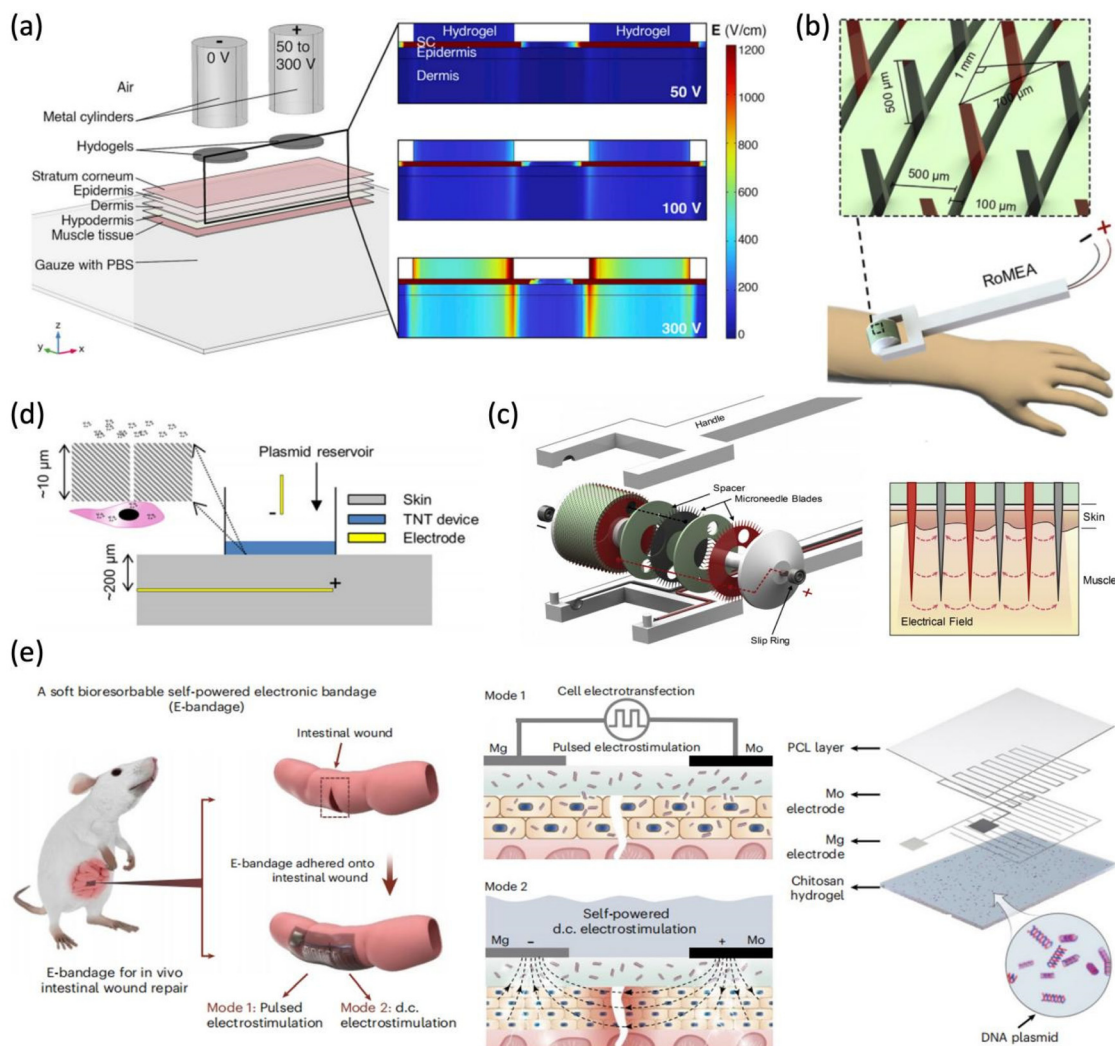


**Fig. 3** Micro/nano-electroporation system for *in vivo* gene therapy. (a) Cascade layers view of the nanocomposite hydrogel drug delivery system and the numerical simulation of electric field distribution during the application of an electric pulse of 50, 100 or 300 V.<sup>73</sup> (b and c) Schematic diagram of the rolling microneedle electrode array (RoMEA) and its exploded view. Microneedle blades are alternately connected to anode (red) and cathode (black).<sup>74</sup> (d) Schematic illustration of the tissue nano-transfection (TNT) device at work. The nanochannels for electroporation are 500 nm in diameter.<sup>72</sup> (e) Fully implantable, biodegradable, self-powered dual electrostimulation E-bandage for intestinal wound healing.<sup>75</sup> Reprinted with permission from ref. 73, © 2024 Elsevier; ref. 74, © 2021 Elsevier; ref. 72, © 2017 Nature; ref. 75, © 2024 Nature.

the accuracy and reliability of the evaluation but also provided strong support for further optimizing electroporation techniques and drug delivery strategies.

Traditional gene therapy often exhibits certain differences in different cell lines, and its operational process is subject to many constraints, which undoubtedly increases the uncertainty and complexity of treatment. In contrast, *in vivo* micro/nano-electroporation devices can overcome these limitations, allowing gene therapy to be applied to a wider range of cell types and diseases.<sup>3,71</sup>

Yang *et al.*<sup>74</sup> combined rolling microneedles with electroporation chips to propose a new type of rolling microneedle electrode array (RoMEA) (Fig. 3b and c). The significant advantage of RoMEA is that it can simultaneously apply an electric field during the rolling process, enabling continuous delivery of siRNA to the target tissue and flexibly adapting to the morphology of different target tissues. In addition, the device uses parallel blades with a microneedle array on the edge as electrodes, effectively penetrating the high-resistance stratum corneum, clearing the path for subsequent delivery. It is worth mentioning that the height of the microneedle electrodes is precisely controlled at 500 micrometers, and the spacing between adjacent anodes and cathodes is 700 micrometers, which can generate a sufficient electric field under the skin to achieve efficient transfection at low voltage. Compared with traditional electroporation methods, RoMEA exhibits greater clinical application potential with its minimally invasive, large-area synchronous rolling and electroporation characteristics.

Gallego-Perez *et al.*<sup>72</sup> developed a tissue nano-transfection (TNT) device for the topical delivery of plasmids. By applying

high-intensity electric fields to aligned nanochannels, they achieved localized and controllable delivery of reprogramming factors into the skin tissue (Fig. 3b). This innovative approach improves the precision and efficiency of delivery. Our team has developed a self-powered electronic bandage that can be precisely applied for targeted gene electroporation and electrical stimulation of intestinal wounds *in vivo*.<sup>75</sup> The device is made of flexible and biodegradable materials, and its unique dual electrical stimulation mechanism significantly promotes the healing process of intestinal wounds (Fig. 3d). Specifically, pulsed electrical stimulation can induce electroporation of epithelial cells, thereby stimulating the expression of healing factors such as epidermal growth factor. At the same time, direct current stimulation further promotes the secretion of healing factors from transfected cells, creating a powerful synergy for healing. The electronic bandage exhibits high transfection efficiency and cell viability in intestinal epithelial cells, effectively promoting the expression of epithelial growth factors during surgery. It is worth mentioning that the self-powered primary battery of this electronic bandage consists of magnesium and molybdenum microelectrodes, achieving self-sufficiency in energy supply and facilitating the extracellular secretion of healing factors. What is even more exciting is that once the wound healing is complete, the electronic bandage can naturally degrade within the organism, eliminating the need for secondary surgical removal.

Despite the diverse form of presentation of the micro/nano-structures for enhancing electroporation performance (Table 1), the common goals in technical innovation include the simplification of system design, the standardization and automation of device fabrication, and the reduction of device

**Table 1** Summary of recently reported micro/nano-electroporation systems with operational information

Micro/nano structure dimensions	Electrical parameters	Cell type	Ref.
An array of triangular shape ITO nano-electrodes with a 70 nm gap	6 V, 20/40 ms, 2/3 pulses	CL1-0 cells, AGS cells, HCT-8 cells, HeLa cells	23
Three nanochip units on one chip (76 mm × 26 mm). Each unit was patterned with 10 000 microwells on the polycarbonate nanomembrane	10 V, 200 pulses	H1975, A549, HCC827	65
16 000 individually addressable and densely packed (>4000 electrodes per mm <sup>2</sup> ) microelectrodes	610 symmetric pulses with 1.22 V amplitude, 1.87 ms	Human dermal fibroblasts	56
Inner/outer diameter 300/500 nm, height 2 μm, and pitch 5 μm, evenly distributed within a 3 mm × 3 mm region	10 V, 400 μs, 20 Hz, 600 cycles	GPE-86 mouse fibroblast cells	69
A PDMS microfluidic channel layer used for cell seeding and introduction of media and reagents, an array of through-hole PDMS culture wells ( <i>n</i> = 400 wells) used to isolate small populations of cells, a nanochannel polycarbonate membrane employed to confine the electric field during pulse application	30 V, 400 pulses, 20 Hz	HeLa cells	70
Functions both as a reservoir for a drug and an electrode for the application of electrical pulses to the skin, by incorporating CNTs into a hydrophilic and biocompatible agarose polymer matrix	300 V, 20 ms, 1 Hz	Mouse skin cells	73
Arrays of ~400–500 nm channels were first defined on the surface of a 200 μm thick double-side polished silicon wafer using projection lithography and DRIE	250 V, 10 ms, 10 pulses	Mouse skin cells	72
The length (height) of the exposed microneedle electrode was only 500 μm, and pitch between the adjacent anode and cathode was 700 μm	50 V, 10 electric pulses (10 ms duration and 1 s interval)	Mouse skin cells, CT26 cell	74
Microelectrode pair (finger width, 200 μm; finger gap, 300 μm)	30 V, 1 ms, 100 pulses	Caco-2 cells, smooth muscle cells, vascular endothelial cells	75

cost. These underlying principles could largely improve the practicality of micro/nano-electroporation devices, ensuring consistent delivery of therapeutic results and reducing the risk of inconsistent treatment effects due to operational differences. These advanced micro/nano-electroporation devices also bear the potential to reduce the cost of gene therapy besides improving its safety and efficiency, allowing more patients to benefit from this effective but costly clinical treatment option.

## 4. The application of micro/nano-electroporation in gene therapy

With the advanced system designs incorporating micro/nano-structures, electroporation technology has found more application in the field of gene therapy. The following section focuses on summarizing the gene delivery and therapeutic results achieved by electroporation-based gene therapy, including, but not limited to those conducted with the devices mentioned above.

### 4.1. *In vitro* gene therapy

**4.1.1. Adoptive immunotherapy.** Adoptive immunotherapy is a therapeutic approach that utilizes the immune system tissues or cells from healthy individuals or the patient's own body to treat diseases. This treatment method involves the collection, isolation, *ex vivo* expansion, and screening of immune cells, which are then reintroduced into the patient's body to

enhance their own immune response and treat various diseases.<sup>76,77</sup>

In addition, adoptive immunotherapy can be further categorized into various types, including engineered T cell receptor therapy, chimeric antigen receptor T cell therapy, natural killer cell therapy, and more. These therapies involve modifying immune cells to enable them to recognize and attack tumor cells with greater precision, thereby improving treatment outcomes.<sup>78,79</sup> However, the modification of immune cells still heavily relies on viral methods, posing safety risks.<sup>80</sup> On the other hand, T cells and NK cells are notoriously difficult to transfect, and current transfection methods have limitations in terms of efficiency.<sup>81,82</sup> Our team<sup>80</sup> reported an innovative and scalable 3D NEP system capable of large-scale transfection, which demonstrated remarkable non-viral cell transfection ability in adoptive immunotherapy. The system utilizes positive dielectrophoresis (DEP) technology to precisely position cells on nanochannels, thereby achieving high-efficiency transfection. To further validate its clinical potential, the researchers tested the system's application in transfecting natural killer cell suspensions and plasmids encoding chimeric antigen receptors (CARs). The results showed a significant improvement in CAR transfection efficiency using the DEP-NEP system, while effectively maintaining cell viability (Fig. 4a and b). Si *et al.*<sup>83</sup> ingeniously utilized the bacteriophage coat protein MS2 to successfully load specific mRNA into exosomes and validated the successful translation of these encapsulated mRNA molecules into functional proteins within recipient cells. By innovatively fusing CD3/CD28 single-

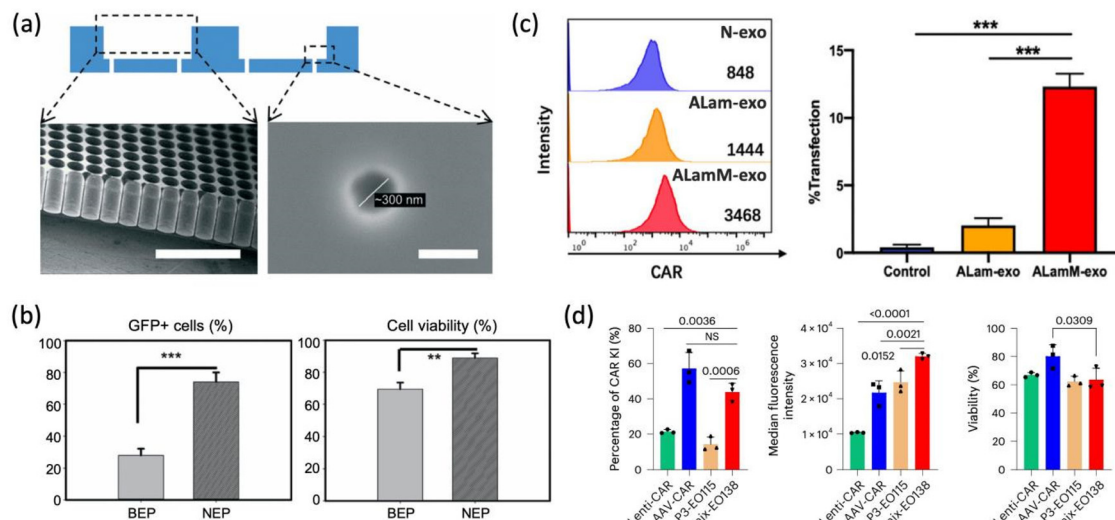


**Fig. 4** The application of micro/nano-electroporation in adoptive immunotherapy. (a) Scanning electron micrographs (SEM) of the nanochannels and microreservoirs of the 3D dielectrophoresis–nanoelectroporation (DEP–NEP) system. Scale bars: 500  $\mu$ m (left), 500 nm (right). (b) Comparison of delivery efficiency (left) and cell viability (right) between BEP and NEP 10 h after CAR plasmid transfection into natural killer cells ( $***p < 0.005$ ,  $**p < 0.01$ ,  $t$ -test).<sup>80</sup> (c) Flow cytometry analysis of mean fluorescence intensity (left) and transfection efficiency (right) of MS2 binding site-fused chimeric antigen receptor (CAR) in T cells 2 days after treatment with N-exo (control exosomes), ALam-exo (exosomes carrying LAMP-2B) or ALamM-exo (exosomes carrying LAMP-2B-MS2).<sup>83</sup> (d) Comparison of lentivirus, AAV or electroporation (P3 or B1mix)-generated CAR T cell efficiency, expression intensity and viability.<sup>84</sup> Reprinted with permission from ref. 80 © 2015 the Royal Society of Chemistry; ref. 83, © 2023 Elsevier; ref. 84, © 2024 Nature.

chain variable fragments with the N-terminus of LAMP-2B, they achieved the expression of these fragments on the outer membrane of exosomes. Furthermore, by inserting MS2 binding sites into the 3' UTR region of CAR genes, they developed engineered exosomes that could be directly used for T cell activation and CAR-T cell preparation (Fig. 4c). Experimental results demonstrated that the CD3/CD28 single-chain variable fragments expressed on exosomes could more easily bind to T cell membranes, and CAR-T cells constructed using this exosome-mediated mRNA delivery exhibited remarkable toxicity to cancer cells. This approach not only provides a safer and more efficient alternative strategy for delivering mRNA to T cells but also opens new avenues for *in vivo* CAR-T cell preparation. This innovative research is expected to have a profound impact in the fields of gene therapy and cell therapy, offering new possibilities for future medical treatments.

An *et al.*<sup>84</sup> discovered that the toxicity observed during electroporation-mediated DNA transfection is mediated by the cGAS-STING pathway. However, this toxic process can be regulated by adjusting the osmotic pressure of the buffer solution used, leading to a significant reduction of the toxicity and a 20-fold improvement in CAR-T cell production efficiency (Fig. 4d). Furthermore, CAR-T cells generated using this optimized method exhibited significantly improved anti-tumor activity compared to the traditional lentivirus method. This finding not only provides a new perspective on understanding the mechanism of DNA transfection *via* electroporation but also offers a new strategy for the efficient production of CAR-T cells.

**4.1.2. RNA interference-based therapy.** RNA interference (RNAi), as a revolutionary approach in the field of life sciences, has undeniable significance and wide-ranging impact. Its basic principle lies in the ability of small double-stranded RNA molecules to specifically degrade or inhibit the expression of homologous mRNA, thereby achieving inhibition or silencing of specific gene expression. As a flourishing gene regulation technology, RNAi has been widely applied in the field of gene therapy, providing new possibilities for the treatment of various diseases.<sup>85–87</sup>

However, the therapeutic potential of RNAi has been severely hindered by the lack of efficient and safe methods for delivery into cells.<sup>88</sup> Patino *et al.*<sup>70</sup> utilized multimodal live-cell analysis device (LCAD) to perform localized electroporation, successfully delivering functional molecules (siRNA) into HeLa cells at multiple time points while preserving cell viability. Temporal changes in gene expression could be observed through multiple molecular delivery experiments, suggesting that RNA plays an important role in regulating gene expression and protein synthesis. In addition, a correlation was found between cellular morphological features and molecular sampling efficiency due to electroporation, which may be related to RNA-mediated intracellular signalling and metabolic regulation. Therefore, RNA interference through electroporation is important for understanding intracellular dynamic processes and molecular regulatory mechanisms (Fig. 5a).

Shokouhi *et al.*<sup>69</sup> utilized electroactive nanoinjection (EIN) for efficient intracellular delivery and gene silencing. Notably,

the platform achieved gene silencing by delivering siRNA targeting TRIOBP, resulting in a gene knockout efficiency of 41.3% (Fig. 5b and c). This achievement further validates its potential application value in the field of gene therapy.

Compared to traditional gene therapy approaches, RNAi technology has shown broad prospects in the field of treatment due to its many advantages, including high specificity, high efficiency, multiplicity of action, and long-lasting effects. By cleverly designing corresponding siRNA, RNAi technology can precisely inhibit or silence disease-related gene expression, thereby achieving significant therapeutic effects.

**4.1.3. Others.** Micro/nano-electroporation for cell transfection offers high efficiency and safety. It enables efficient delivery of substances while preserving cell integrity, thereby significantly enhancing therapeutic effectiveness. Compared to transfection methods such as viral vectors, micro/nano-electroporation is easier to control and offers increased safety and reliability, greatly reducing potential treatment risks. These characteristics have made it highly favored and an important technical approach in the field of gene therapy.<sup>89–91</sup>

Pathak *et al.*<sup>32</sup> optimized the intracellular delivery of large proteins, protein–nucleic acid conjugates, and Cas9–ribonuclease complexes using a nanochannel-based electroporation platform (Fig. 6a). They achieved high delivery efficiencies of 75.38% for large proteins such as  $\beta$ -galactosidase (with a molecular weight of 472 kDa), 80.25% for protein–nucleic acid conjugates such as proteinaceous nucleic acids (with a molecular weight of 668 kDa) and accomplished 60% knockout efficiency and 24% knock-in efficiency for Cas9–ribonucleoprotein complexes (with a molecular weight of 160 kDa). It is worth mentioning that the local electroporation platform they employed successfully retained the functionality of these biomolecules during the delivery process, achieving the largest protein delivery reported to date.

In addition, micro/nano-electroporation technology has demonstrated powerful versatility. It can be used not only for gene delivery but also for the delivery of proteins, antibodies, and various other substances. It is applicable to a wide range of gene therapy scenarios, providing more options and possibilities for the development of treatment strategies.<sup>30,32,33</sup> Duckert *et al.*<sup>56</sup> utilized their HD-EP platform to identify the optimal electroporation parameters and achieved safe, precise and efficient transfection of primary cells. They successfully delivered Cas9-GFP single-guide RNA ribonucleoprotein complexes (RNP, with a molecular weight exceeding 200 kDa), a 70 kDa fluorescent dye, and mCherry-encoding mRNA (1 kB) respectively into primary human dermal fibroblasts, reaching over 90% cell viability in all cases (Fig. 6b). The exact overlap of the transfected (fluorescent) cells with the activated micro-electrodes (indicated by white dots) demonstrates the high spatial precision of using MEA in transfection. The development of HD-EP with MEA technology provides an insight for tackling the issue of hard-to-transfet cells such as T cells and NK cells and improving transfection safety and efficiency for gene therapy. Yan Sheng *et al.*<sup>92</sup> have developed a cell delivery and extracellular RNA analysis platform based on nano-electro-

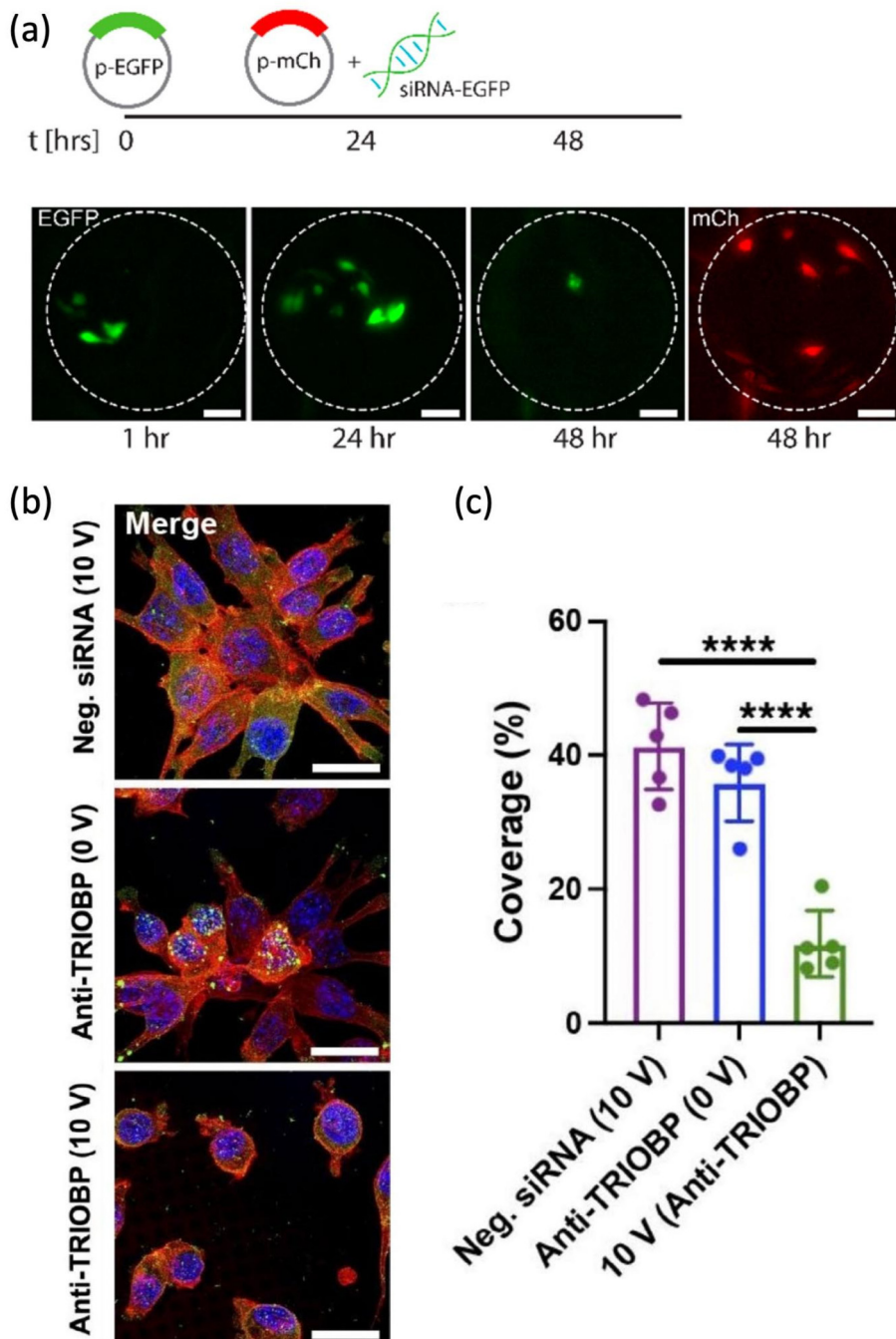


**Fig. 5** The application of micro/nano-electroporation in RNA interference-based therapy. (a) Schematic of the multitime-point delivery procedure (a first delivery of EGFP plasmids and a codelivery of EGFP-siRNA and mCherry plasmids 24 h later into the same group of cells) implemented with the LCAD and the fluorescence micrograph characterization of gene expression after the multitime-point delivery.<sup>70</sup> (b) Merge-channel confocal micrographs of mouse fibroblast (GPE-86) cells on the ENI platform 24 h after nanoscale-EP (10 V; 400  $\mu$ s; 20 Hz; 600 cycles) delivery of control siRNA (Neg. siRNA) or TRIOBP-targeting siRNAs (Anti-TRIOBP). The successful delivery of TRIOBP-targeting siRNAs leads to knockdown of TRIOBP, which disrupts actin skeleton reorganization and thus alters cell morphology and hinders cell migration and proliferation. Blue: Hoechst (nuclei); red: phalloidin (F-actin); green: TRIOBP antibody (TRIOBP). (c) Statistical analysis of area coverage by cells resulting from (b).<sup>69</sup> Reprinted with permission from ref. 70 © 2022 American Chemical Society; ref. 69, © 2023 Nature.

poration technology to achieve precise cellular-level drug delivery and real-time potency detection (Fig. 6c). In their Cell Electroporation and Analysis Device (CEAD), the clever combination of nanochannels and microarrays allows for the precise

positioning of individual cells within the nanochannels, enabling rapid and accurate intracellular delivery of drug molecules. This discovery not only brings breakthroughs in cellular-level drug delivery but also has far-reaching impli-

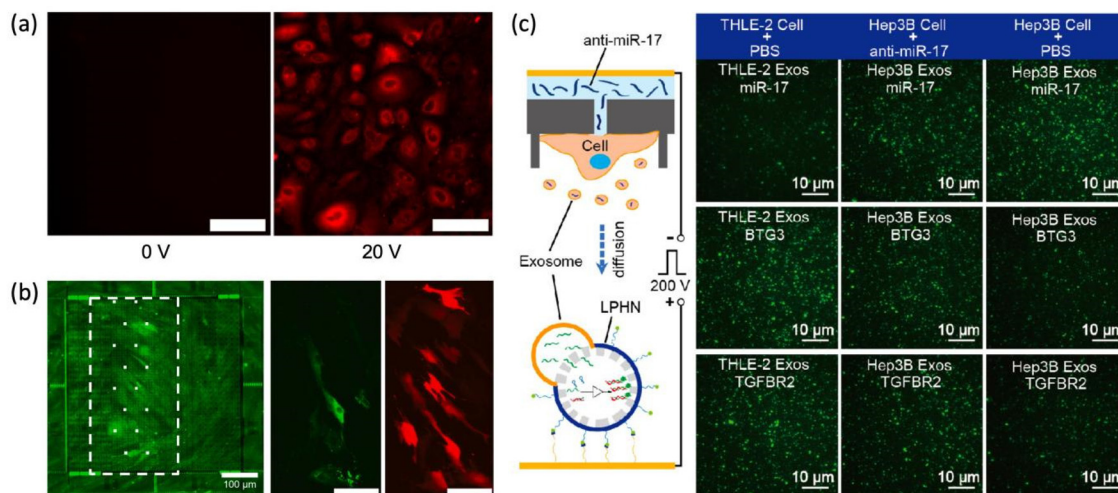


**Fig. 6** The application of micro/nano-electroporation in *in vitro* gene therapy. (a) Representative fluorescent micrographs of HeLa cells incubated with AF-647-tagged  $\beta$ -gal (472 kDa) proteins (left, control) and after electroporation-induced delivery of AF-647-tagged  $\beta$ -gal (right) with the localized electroporation device (LEPD). Scale bars: 70  $\mu$ m.<sup>32</sup> (b) Fluorescence micrographs of primary human dermal fibroblasts after the delivery of Cas9-GFP ribonucleoprotein complexes (RNPs, >200 kDa) (left), fluorescein-labelled dextran (70 kDa) (middle) or mCherry-encoding mRNA (right) on the HD-EP chip with optimized electroporation conditions. Dashed rectangle indicates the area displayed in the other two panels (white dots indicate the activated microelectrodes during transfection). The area is centered around the 45.5  $\text{mm}^2$  electrodes, which was the optimal electrode size used to deliver larger molecules while maximizing cell survival. Scale bars: 100  $\mu$ m.<sup>56</sup> (c) Schematic diagram of anti-miR-17 transfection and exosome detection by the cellular-nanoporation and exosome assessment device (CEAD). Total internal reflection fluorescence (TIRF) micrographs of miR-17, BTG3 mRNA, and TGFBR2 mRNA expression in THLE-2 exosomes (left column), Hep3B exosomes (middle column), and Hep3B exosomes (right column) using dose treatment of PBS, anti-miR-17, and PBS, respectively.<sup>92</sup> Reprinted with permission from ref. 32 © 2023 American Chemical Society; ref. 56, © 2022 Elsevier; ref. 92 © 2019 American Chemical Society.

cations for further advancements and improvements in gene therapy, gene editing, and other related fields.

#### 4.2. *In vivo* gene therapy

**4.2.1. *In vivo* delivery of therapeutic genes.** For gene therapy, various types of therapeutic genes can be efficiently delivered into cells through *in vivo* electroporation, thereby regulating cell growth, differentiation, and tissue functions, with the aim of treating diseases or repairing damaged tissues.<sup>72,93–95</sup> Yang *et al.*<sup>74</sup> proposed and validated the strategy of RoMEA-mediated *in vivo* transdermal delivery of siRNA. Blocking the PD-L1/PD-1 immune checkpoint pathway is the most representative approach for tumor immunotherapy in clinical treatment. Based on the optimal parameters of RoMEA, Yang and colleagues selected siRNA (siPD-L1) that inhibits PD-L1 expression and monoclonal antibody (PD-1 mAb) that antagonizes PD-1 for study in the B16-F10 melanoma mouse model. The results showed that the use of siPD-L1 alone or in combination with PD-1 mAb can effectively inhibit tumor growth and prolong animal survival (Fig. 7a–c). Gallego-Perez *et al.*<sup>72</sup> reported successful *in vivo* cell reprogramming through TNT-based topical delivery of reprogramming factor (Etv2, Foxc2 and Fli1 (EFF))-encoded plasmids into murine skin fibroblasts. The efficient electrotransfection resulted in remarkable signs of dermal cell reprogramming to endothelial cells within 4 days of transfection (*i.e.*, within a week of the transection of femoral artery). The consistent expression of the reprogramming factors led to fast

reconstruction of the transected femoral vasculature and notably increased limb reperfusion within 14 days, successfully reviving the injured limb in a timely manner (Fig. 7d and e). With this technology, a single non-invasive procedure can convert skin cells into foundational components of any organ, offering tremendous potential for innovative applications in the field of medicine. Our team has innovatively developed a self-powered electronic bandage with both flexibility and biodegradability, specifically designed for targeted gene electrotransfection and electrical stimulation of intestinal wounds *in vivo*.<sup>75</sup> This electronic bandage significantly enhances the generation of growth factors in the local extracellular environment, effectively promoting proliferation in various layers of intestinal tissue, including epithelial and muscular tissue (Fig. 7f and g). Compared to traditional absorbable sutures, the electronic bandage demonstrates significant advantages in the postoperative recovery process. It not only reduces the risk of postoperative hyperplasia and obstruction but also promotes faster and more effective weight recovery in mice. Furthermore, the electronic bandage further promotes tissue healing by increasing the number of beneficial bacteria, thereby improving the overall health of the intestines. This innovative achievement not only provides a new solution for the treatment of intestinal wounds but also offers potential insights for the future development of the medical field.

**4.2.2. Gene editing.** Gene editing is an emerging technology that enables precise modifications of specific target genes in an organism's genome. This technique relies on genetically

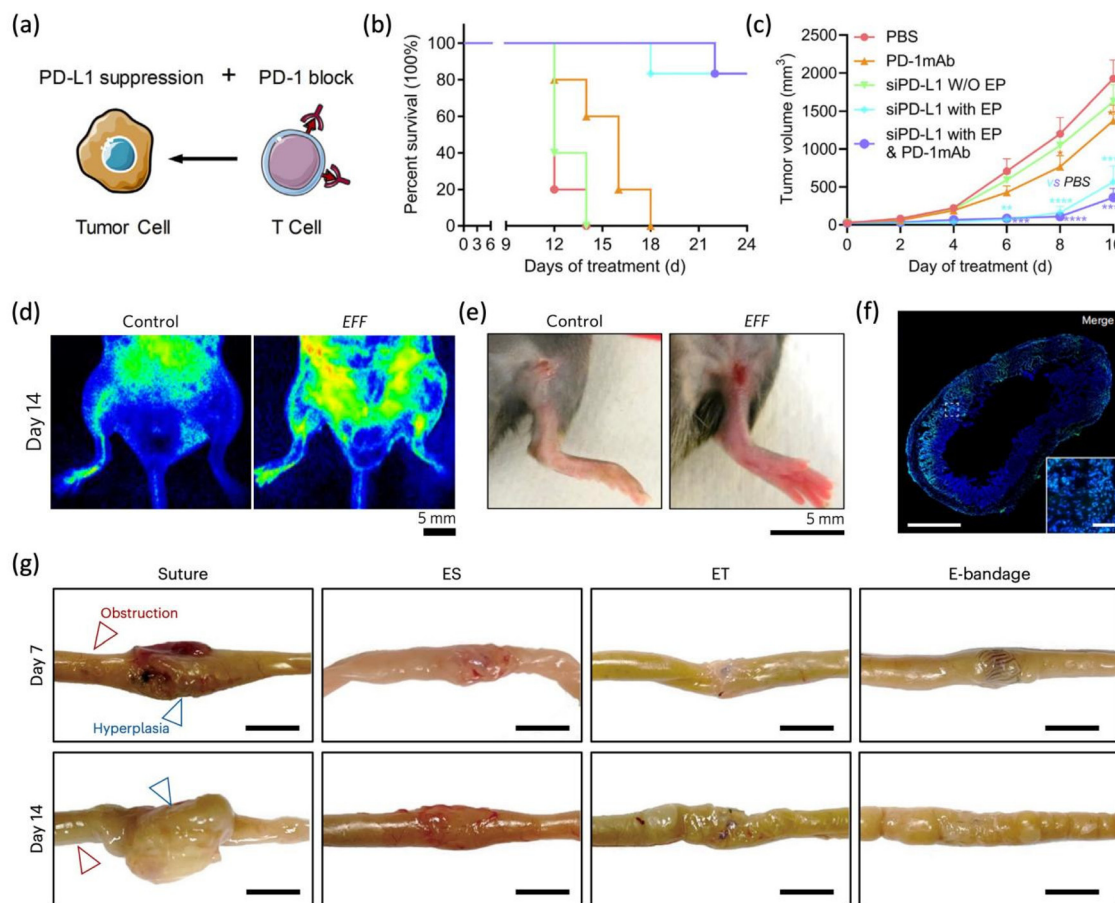


**Fig. 7** Therapeutic effects of gene therapy delivered by *in vivo* micro/nano-electroporation systems. (a) Conceptual illustration of the immunotherapy strategy intended with the RoMEA-mediated PD-L1 knockdown. (b and c) The survival rates (b) and tumor growth curves (c) of the early-stage melanoma mice models during the immunotherapy treatment course. PD-1 mAb: anti-PD-1 monoclonal antibody; siPD-L1: anti-PD-L1 siRNA; EP: electroporation implemented with RoMEA.<sup>74</sup> (d) Representative IVIS images showing the significantly increased limb reperfusion on day 11 after the TNT-mediated reprogramming of dermal cells into induced endothelial cells (iECs) (day 14 after femoral artery transection). EFF: reprogramming factors Etv2, Foxc2 and Fli1 delivered by TNT. (e) Macroscopic view of the healthy-looking limb after TNT-based EFF delivery in comparison to the control limb showing pronounced signs of tissue necrosis (day 14 after femoral artery transection).<sup>72</sup> (f) Merge-channel fluorescence micrograph of the transverse view of the electrotransfected intestinal section by the E-bandage 48 h after implantation. Blue: DAPI (nuclei); green: GFP (EGF expressed from transfected plasmids encoded with EGF and GFP). Scale bars: 1 mm (left); 200  $\mu$ m (right). (g) Representative images of the occurrence of hyperplasia and obstruction in mice treated with suture-based wound closure surgery (Suture), E-bandage implantation but implementing only direct current electrostimulation (ES), E-bandage implantation but implementing only electrotransfection of EGF-encoded plasmids (ET), or E-bandage implantation implementing dual-mode electrostimulation (E-bandage) on day 7 and day 14 after implantation. Scale bars: 5 mm.<sup>75</sup> Reprinted with permission from ref. 74, © 2021 Elsevier; ref. 72, © 2017 Nature; ref. 75, © 2024 Nature.

engineered nucleases, which generate site-specific double-strand breaks at specific locations in the genome, inducing the organism to repair these breaks through non-homologous end joining or homologous recombination.<sup>96–98</sup>

CRISPR-Cas9 is a third-generation gene editing technology introduced after ZFN and TALENs. It is characterized by its high efficiency, simplicity, and low cost, making it the mainstream gene editing system today.<sup>99,100</sup> Currently, gene therapy approaches based on CRISPR-Cas9 have been successfully used in gene therapy trials for various monogenic/multigenic genetic diseases, tumors, and viral infectious diseases.<sup>101–104</sup> However, efficiently delivering CRISPR-Cas9 into cells within the body for gene editing remains a pressing challenge that needs to be addressed.

Wan *et al.*<sup>105</sup> ingeniously bypassed the complex process of plasmid transfection by optimizing electroporation and directly loaded Cas9 RNPs into exosomes (Exosome<sup>RNP</sup>) derived from hepatic fibroblasts (Fig. 8a and b). Exosome<sup>RNP</sup> exhibits remarkable therapeutic potential in mouse models of acute liver injury, chronic liver fibrosis, and hepatocellular carcinoma by targeting p53 up-regulated modulator of apoptosis (PUMA), CcnE1, and K (lysine) acetyltransferase 5 (KAT5). This study not only successfully constructed gene-editing nanoparticles based on exosomes, achieving efficient delivery of RNP to target cells, but also achieved significant results in terms of gene editing efficiency. This characteristic not only avoids off-target gene editing in non-target organs but also greatly enhances the safety and precision of *in vivo* genome editing.

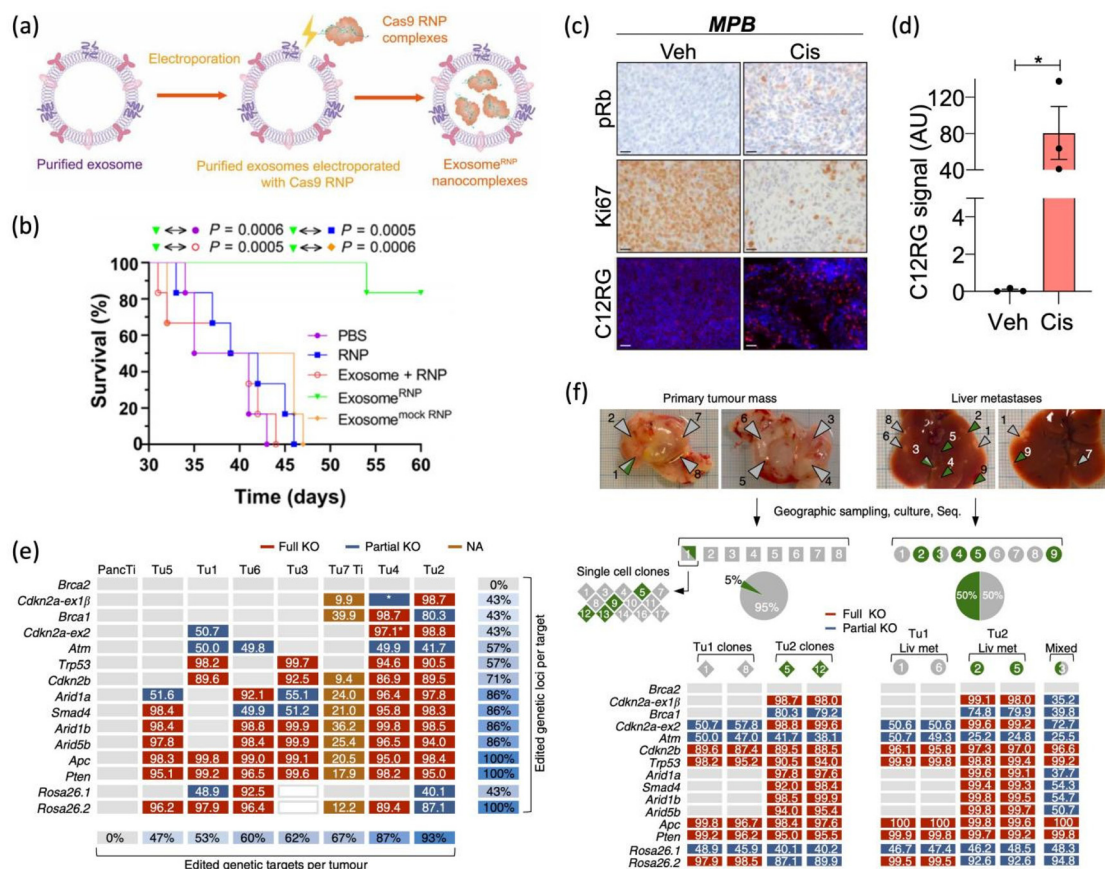


**Fig. 8** The application of micro/nano-electroporation in gene editing. (a) Schematic illustration of electroporation-mediated delivery of Cas9 RNPs into exosomes for subsequent *in vivo* delivery of the therapeutic agent. (b) Survival rates of mice with orthotopic hepatocellular carcinoma after the *in vivo* delivery of the engineered exosomes (Exosome<sup>RNP</sup>) in comparison to those of the control group mice.<sup>105</sup> (c) Immunohistochemical staining of phospho-Rb (pRb) and Ki67 and staining of C12RG, a fluorogenic substrate for senescence-associated  $\beta$ -galactosidase (SA- $\beta$ -gal) activity, of subcutaneously transplanted tumors treated with vehicle or cisplatin. MPB indicates tumors developed after electroporation-mediated delivery of plasmid DNA encoding CRISPR–Cas9 constructs and vectors coexpressing sgRNAs for MYC, Trp53 and Brca1. Scale bars: 20  $\mu$ m. (d) Quantification of SA- $\beta$ -gal activity reflected by C12RG levels from (a).<sup>106</sup> (e) Target site mutations in induced primary tumors (pancreatic ductal adenocarcinoma, PDAC) after electroporation-mediated CRISPR/Cas-editing of 15 cancer-related genes. Numbers in boxes indicate for each target site mutant read frequencies (MRFs; defined as the fraction of mutant sequence reads/all reads at individual target loci). (f) Phylogenetic tracking of CRISPR/Cas9-induced metastatic PDAC.<sup>107</sup> Reprinted with permission from ref. 105, © 2022 Science; ref. 106, © 2022 PNAS; ref. 107, © 2016 Nature.

By delivering plasmid DNA encoding CRISPR–Cas9 constructs and transposon vectors coexpressing Trp53-targeting single-guide RNAs (sgRNAs) targeting MYC, Trp53, and Brca1 into the ovaries and fallopian tubes with electroporation techniques, Paffenholz *et al.*<sup>106</sup> observed a significant increase in sensitivity of homologous recombination-deficient HGSOC tumors to platinum-based chemotherapy drugs (Fig. 8c and d). This finding provides important clues for a deeper understanding of the senescence mechanisms in HGSOC tumors and lays a solid foundation for the development of more effective tumor treatment strategies.

Maresch *et al.*<sup>107</sup> delivered the CRISPR/Cas9 system into mouse pancreatic cells using electroporation, enabling simultaneous editing of 15 cancer-related genes in individual cells to initiate tumor formation (Fig. 8e and f). With the high efficiency of delivering multiple genes in the same cells, Maresch and colleagues discovered similar metastatic pattern

from primary tumors with similar mutation profiles. This technique allows for more efficient investigation of gene function and interactions, opening new avenues for disease treatment and prevention. Delivering Cas9 ribonucleoprotein (RNP) complexes as an efficient gene editing approach offers significant advantages. It effectively avoids the cellular transcription and translation processes required for delivering Cas9 DNA/mRNA, thereby reducing potential immunogenicity and off-target effects. However, the challenge lies in the difficulty of Cas9 RNP crossing the cell membrane due to its large molecular weight, making it challenging for existing delivery systems to effectively encapsulate it. This has become a bottleneck for its translational applications.<sup>108,109</sup>

Overall, gene editing technology is indeed a revolutionary breakthrough that greatly expands our understanding and manipulation of the fundamental building blocks of life. By precisely modifying and controlling genes, gene editing holds

the potential to bring forth more possibilities for human health and the development of biotechnology in the future.

**4.2.3. Gene therapy mediated by micro/nano-electroporation engineered EV.** EVs, as critical mediators of intercellular communication and material transfer, with their unique membrane structure, low immunogenicity, and manipulatable surface and interior contents, serve as ideal carriers for drug delivery and gene therapy. However, effectively loading drugs into EVs has been a technical challenge.<sup>110–112</sup>

The emergence of micro/nano-electroporation technology provides an effective solution to this challenge. Micro/nano-

electroporation technology has enabled the discovery of elevated production of EVs loaded with transfected cargos from the transfected cells. This discovery thus opened up a wide range of new possibilities in the field of gene therapy. Yang *et al.*<sup>93</sup> employed cellular nano-electroporation (CNP) methods to efficiently produce exosomes enriched with therapeutic mRNA and targeting peptides. These exosomes possess the ability to cross the blood–brain barrier or blood–brain tumor barrier, enabling precise targeted delivery to tumors (Fig. 9a and b). Compared to traditional bulk electroporation and other exosome production strategies, cellular nano-electropora-

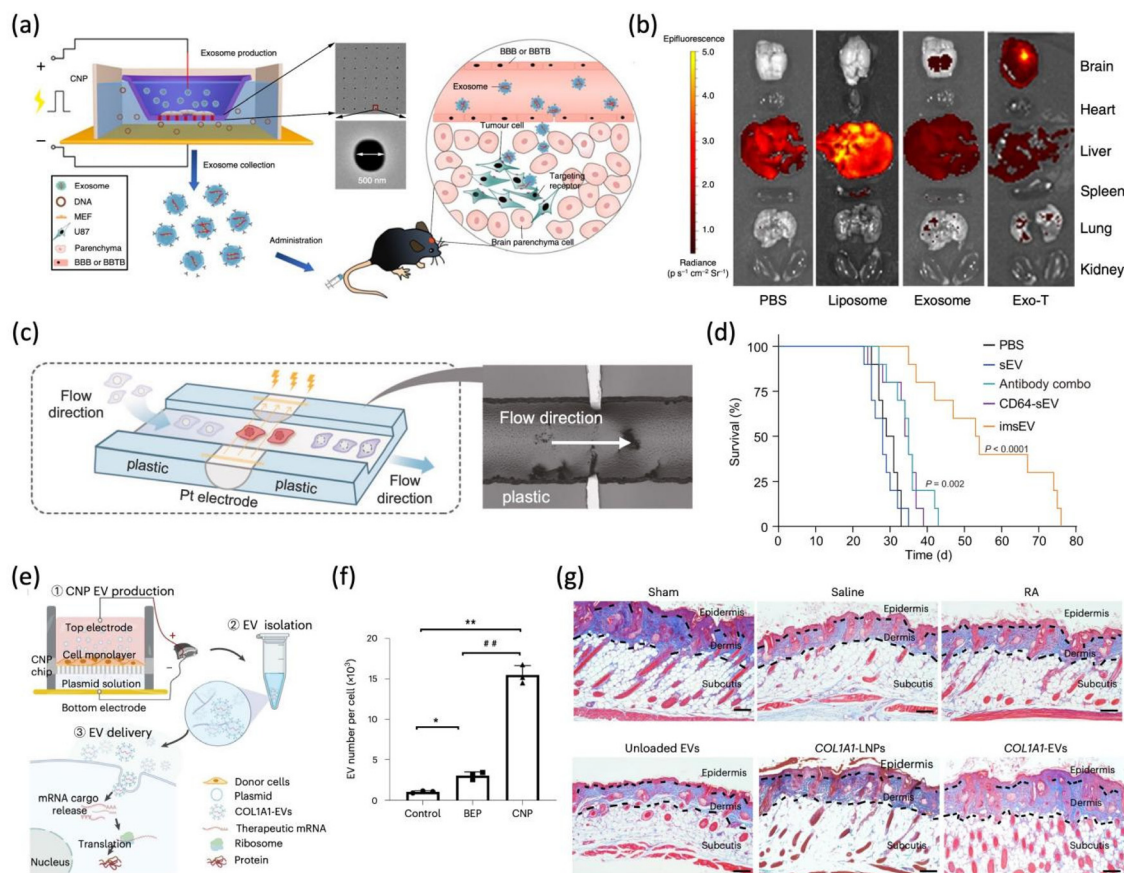


**Fig. 9** The application of micro/nano-electroporation in engineering EVs for *in vivo* gene therapy. (a) Schematic illustration of the generation of EVs loaded with mRNAs transcribed from exogenous nucleic acids transfected with cellular nanoporation (CNP), and the subsequent application of these EVs for tumor-targeted delivery through the blood–brain barrier (BBB) or blood–brain tumor barrier (BBTB). SEM inset: the nanochannel array and an individual nanochannel in the CNP system, with channel diameter of 500 nm. (b) Inhibition of glioma tumor growth in mice by CNP-generated therapeutic exosomes. Exosome: non-engineered exosomes; Exo-T: CNP-generated exosomes containing PTEN mRNA with surface modification with murine glioma-targeting peptide CREKA; E-Exo-T: empty Exo-T without PTEN mRNA; Liposome: PEG-liposome nanoparticles.<sup>93</sup> (c) Schematic diagram and SEM image of the nanosecond pulse electroporation (nsEP) system for small EV (sEV) generation. (d) Survival rates of mice with glioblastoma after treatment with nsEP chip-generated therapeutic sEVs. sEV: nsEP chip-generated sEVs containing IFN- $\gamma$  mRNAs derived from the transfected plasmids; CD64-sEV: sEVs overexpressing CD64, an exosomal surface protein that can recruit IFN- $\gamma$  mRNAs into the sEVs; imsEV: CD64-sEVs with murine glioblastoma-targeting antibodies (anti-CD71 and anti-PD-L1) docked onto CD64; Antibody combo: tail vein injection of anti-CD71 and anti-PD-L1.<sup>113</sup> (e) Schematic diagram of CNP-generated EVs loaded with COL1A1 mRNA for targeted nucleic acid delivery. (f) Comparison of EV yield per cell (neonatal human dermal fibroblasts) over 24 h after PBS incubation (Control), cargo-less BEP or cargo-less CNP. (g) Masson's trichrome staining showing the rejuvenation (i.e., higher collagen content and greater skin thickness) of murine skin tissue treated with CNP-generated therapeutic EVs in a UV-irradiation photoaging model. Blue stains represent collagen. Sham: wildtype murine skin; Saline: saline control in the photoaging model; RA: topical application of retinoic acid; Unloaded EVs: EVs generated from cargo-less CNP; COL1A1-LNPs: COL1A1-loaded lipid nanoparticles; COL1A1-EVs: CNP-generated therapeutic EVs loaded with COL1A1 mRNAs. Scale bars: 200  $\mu$ m.<sup>114</sup> Reprinted with permission from ref. 93, © 2020 Nature; ref. 113, © 2023 Nature; ref. 114, © 2023 Nature.

tion technology significantly enhances exosome yield, with increases of up to 50-fold. Moreover, exosomes prepared using this technique exhibit a remarkable increase in the content of mRNA transcripts, exceeding 103-fold. Dong *et al.*<sup>113</sup> utilized a microfluidic electroporation method to dock different targeting ligands onto the surface of mRNA-loaded small extracellular vesicles (sEVs). In this approach, a combination of nanosecond and millisecond pulses generated a large quantity of sEVs loaded with IFN- $\gamma$  (Fig. 9c and d). CD64 molecule, serving as a targeting ligand adapter, facilitated the preferential targeting of immunogenic sEVs to glioblastoma cells and exerted potent anti-tumor activity *in vivo*. The drug-loaded exosomes can subsequently be used for cell therapy or drug delivery. They can target specific cells or tissues, enabling precise treatment. Additionally, exosomes possess inherent biocompatibility and low immunogenicity, enhancing their safety and efficacy in biomedical applications. You *et al.*<sup>114</sup> developed an mRNA loading technique based on cellular nanoelectroporation, enabling the loading of COL1A1 mRNA into EVs at a copy number of exceeding traditional methods by 1000-fold (Fig. 9e–g). Additionally, the researchers ingeniously designed microneedle patches to precisely deliver COL1A1-EV MN patches into the dorsal skin of mice. Experimental results demonstrated that this technique allowed for more uniform rejuvenation of the mouse skin surface, showcasing tremendous potential in treating aging skin or protein loss caused by other diseases.

## 5. Electroporation for gene therapy in clinical settings

In recent years, remarkable progress has been made in the research of using electroporation technologies for clinical medicine, demonstrating tremendous potential.<sup>115</sup> Gene electrotransfer (GET) as a major branch of electroporation therapy (EPT), which uses high-intensity, short-duration electric pulses to increase the permeability of cell wall for enhanced uptake of chemotherapeutic drugs, genes or vaccines in clinical settings, has become a relatively mature technology.<sup>116,117</sup> Some FDA-approved GET devices in current clinical practice include CELLECTRA®, TriGrid™, and MedPulser™ (Fig. 10a–c). Among them, CELLECTRA® and TriGrid™ are designed for delivering subcutaneous and intramuscular DNA vaccine shots, respectively, and thus are equipped with hand-held applicators housing disposable vaccine cartridges, and shorter syringe electrodes (Fig. 10d). MedPulser™ systems on the other hand, are equipped with longer syringe electrode array applicator for delivering intratumoral therapies (Fig. 10e).<sup>118</sup> The design that holds in common is the ~0.5 cm space between the arrayed electrodes for implementing an applied electric field with tolerable strength, ensuring application safety. In comparison to traditional injection methods, GET not only significantly enhances the number of transfected cells and the intensity of gene expression but also enables co-trans-

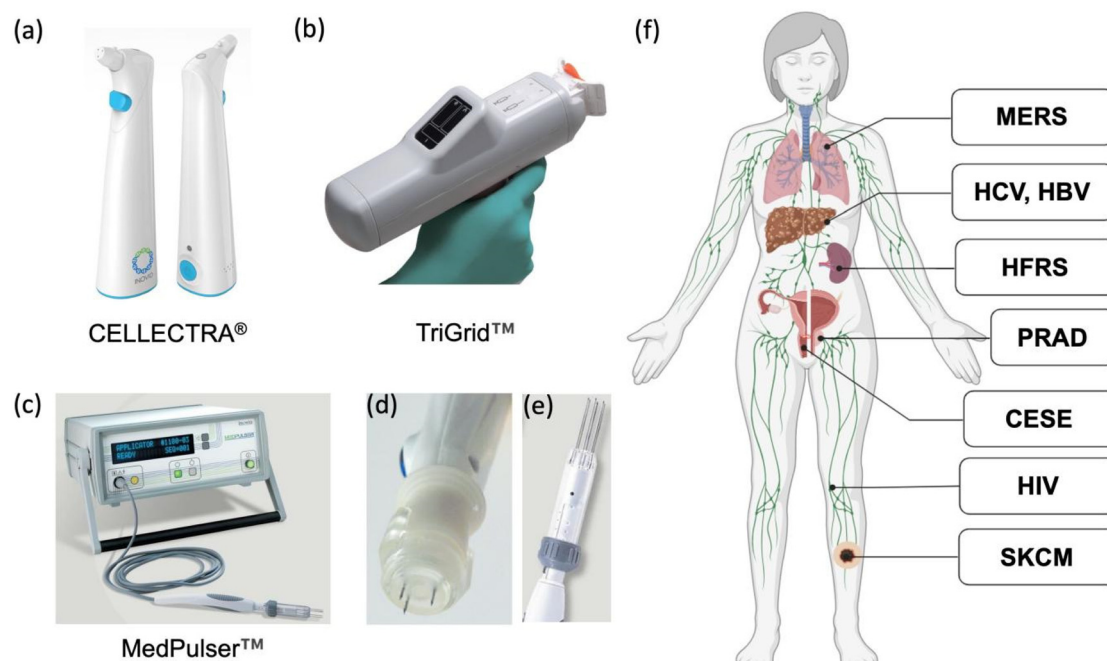


**Fig. 10** GET devices and their applications in clinical practice. (a) CELLECTRA® system (<https://inovio.com/dna-medicines-technology/>). (b) TriGrid™ system (<https://ichorms.com/>). (c) MedPulser system (<https://inovio.com/dna-medicines-technology/>). (d and e) Syringe/electrode array applicator of CELLECTRA® (d) and MedPulser™ (e). (f) The application of GET in treating various diseases (MERS: Middle East respiratory syndrome; HCV: hepatitis C virus; HBV: hepatitis B virus; HFRS: hemorrhagic fever with renal syndrome; PRAD: prostate cancer; CESE: cervical carcinoma; HIV: human immunodeficiency virus; SKCM: skin cutaneous melanoma).

**Table 2** Application of GET in vaccine development

Disease	DNA	Detail	Phase	Additional information	Clinical trial ID	Specificities	Ref.
Hepatitis C	VGX-6150	pDNA targeting the antigens NS3/4A	I	In conjunction with interferon, ribavirin; delivered with CELLECTRA®	NCT02027116	5/12 patients showed a significant decrease in serum HCV RNA from 2 to 10 weeks old; 6/8 completely cured	130
Hepatitis B	HBV DNA vaccine	HBV envelope- and nucleocapsid-based DNA vaccines	II	In conjunction with lamivudine	NCT01487876	The proportion of HBV DNA inhibition and the positive reaction rate of T cells significantly increased	131
AIDS	Nef/tat/vif (clade B) and Env (clades B and C) PENNVAAX-GP	HBV-1 nef/tat/vif, env pDNA vaccine + rVSV HIV envC Mixture of pDNA encoding HIV-1 env/gag/pol	I/II	—	NCT02654080	The vaccine elicited Env-specific CD4 <sup>+</sup> T cell responses in over 80% of participants and CD8 <sup>+</sup> T cell responses in 30% of participants	132
HIV-MAG		Mixture of pDNA encoding HIV-1 gag/pol and HIV-1 nef/tat/vif, env	I	In conjunction with plasmid encoding hIL-12; delivered with CELLECTRA®	NCT02431767	The response amplitude of IgG binding antibodies targeting the common envelope of gp140 is significantly increased	133
Hemorrhagic fever with nephrotic syndrome	HTNV and PUUV DNA vaccines	Plasmid expressing two of the three gene segments of HTNV and PUUV (the M and S segments)	I	Delivered with TriGrid™	NCT01266616	HIV-1 MAG/low-dose IL-12 DNA vaccine enhances CD4(+) rather than CD8(+) T cell responses to multiple HIV-1 antigens	134
Middle East Respiratory Syndrome (MERS) Prostatic cancer	GLS-5300 pVAXrcPSAv531	Plasmid expressing two of the three gene segments of HTNV and PUUV (the M and S segments)	I	Delivered with TriGrid™	NCT01502345	Both vaccines produce neutralizing antibodies when administered alone or in combination	135
Cervical carcinoma	VGX-3100	DNA vaccine expressing a full-length MERS coronavirus S-glycoprotein antigen	I	Delivered with CELLECTRA®	NCT02670187	More than 85% of participants can detect an immune response after two consecutive vaccinations; persistent presence during 1-year follow-up	137
Cervical carcinoma melanoma	GX-188E	DNA encoding E6 and E7 oncogenes of HPV types 16 and 18	I	Delivered with CELLECTRA®	NCT00859729	There are no obvious systemic side effects, and some patients develop T cell immune responses	138
	pINGmutYr	DNA vaccine encoding E6 and E7 oncogenes of HPV types 16 and 18	I	Delivered with TriGrid™	NCT01304524	Effectively inducing HPV specific CD8(+) T cell response	139
		DNA vaccine encoding the melanosomal antigen tyrosinase	I	Delivered with TriGrid™	NCT01634503	After 36 weeks of treatment, the pathological regression rate significantly increased	140
					NCT00471133	88.89% of patients exhibit strong HPV specific CD8 <sup>+</sup> T cell responses; 77.78% of patients experienced complete regression of lesions and virus clearance within 36 weeks of follow-up	141
						Among patients with the highest dose, 40% exhibited arginine responsive CD8 <sup>+</sup> T cell responses; 14% of patients with various doses experienced arginine responsive CD8 <sup>+</sup> IFN- $\gamma$ <sup>+</sup> Increased T cells	142

fection, resulting in a dramatic increase in gene expression levels by 100 to 1000-fold.<sup>119,120</sup> These advantages have positioned GET as a highly promising novel gene delivery tool with immense potential in the field of gene therapy.

### 5.1. DNA vaccine

GET plays a crucial role in the vaccine development for various diseases (Fig. 10f).

In the process of vaccine development, GET has the capability to directly deliver DNA vaccines into host cells, significantly enhancing the cellular uptake efficiency of DNA or RNA vaccines. This effectively stimulates a stronger immune response, thereby greatly enhancing the vaccine's effectiveness and bringing about a revolutionary breakthrough in the field of vaccines.<sup>121–123</sup> Table 2 provides an overview of the current practical applications of GET in vaccines, showcasing its outstanding performance in enhancing vaccine efficacy. Through the application of GET technology, it is expected that more efficient and safe vaccines can be developed, making a significant contribution to the field of human health.

### 5.2. Tumor treatment

In the field of cancer treatment, GET technology has demonstrated remarkable therapeutic potential by delivering plasmids encoding specific proteins. This approach allows for the direct transfer of therapeutic genes into tumor cells, thereby exerting direct or indirect anti-tumor effects.<sup>124–126</sup>

Using GET technology, the successful delivery of the IL-12 gene into tumor cells has been achieved, effectively activating T cells, NK cells, and tumor-infiltrating lymphocytes in the tumor microenvironment. This has significantly inhibited tumor growth and induced apoptosis in tumor cells. Further *in vivo* studies have demonstrated that the efficient delivery of IL-2 through GET can effectively eliminate metastatic melanoma and prevent its recurrence.<sup>127</sup> In a clinical study involving 24 patients with metastatic melanoma, two patients achieved complete remission of metastatic tumors after receiving GET treatment. Additionally, eight patients experienced partial remission or stabilization of the disease, indicating positive effects.<sup>128</sup> Antiangiogenic metarginine peptide (AMEP), as a novel anticancer agent, demonstrates powerful anti-tumor potential through its unique mechanism of targeting tumor proliferation and neovascularization. By binding to  $\alpha\beta 3$  and  $\alpha 5\beta 1$  integrins, it effectively inhibits tumor growth. In a comprehensive study focusing on advanced cutaneous metastatic melanoma, AMEP plasmids were precisely delivered into the tumor using GET technology on day one and day eight. After 29 days of evaluation, no severe adverse reactions were observed during the treatment, and successful expression of AMEP mRNA was detected in most lesions. More excitingly, all five treated lesions showed cessation of growth, whereas in the control group, four out of five lesions showed a diameter increase of over 20%. These research findings indicate that the delivery of AMEP into cutaneous melanoma using GET technology is not only safe and feasible but also provides significant local therapeutic benefits. These encouraging results strongly

support the application of GET in tumor treatment and pave the way for the development of future cancer treatment strategies.<sup>129</sup>

In summary, the progress of micro/nano-electroporation technology in the field of clinical gene therapy has fully demonstrated its immense potential. By achieving precise and efficient gene delivery, driving translational research, and providing novel strategies for treating various diseases, this technology is at the forefront of a profound transformation in the field of gene therapy.

## 6. Summary and future perspectives

Micro/nano-electroporation technology, through the transient application of electric fields in a micro/nanostructure-confined space, can precisely disrupt the cell membrane, allowing desired cargos to enter the cells smoothly. Compared to traditional circulation-based gene delivery methods, locally administrating micro/nano-electroporation approaches exhibit unique advantages such as safety, precision, and controllability. To further exert these advantages for gene therapy, several challenges still need to be addressed.

An essential aspect of improving micro/nano-electroporation-based gene delivery relies on the thorough understanding of the intrinsic mechanisms of electro-perforating living cells or tissues to establish a systematic approach for finding the balance between electroporation safety and efficiency. Detailed mechanisms at the cellular and molecular levels, such as plasma membrane dynamics and the intracellular trajectory of delivered cargos, need to be analyzed in depth.<sup>143</sup> Based on different application scenarios, personalized adjustments can be made, including adjusting the electrode configuration and parameters of the electric pulses (*i.e.*, field strength, pulse duration, pulse number, and frequency), aiming for optimal treatment outcomes in different organs and tissues, such as the skin, liver, and muscles. However, these parameters are interrelated and mutually influenced, making their adjustment quite complex. More systematic and omics-level studies are in need to provide us with new perspectives and solutions to maximize delivery efficiency while maintaining electroporation safety on both cellular and organism levels.

Another equally important and interrelated aspect is the innovation and improvement in the design and fabrication procedure of micro/nano-electroporation devices. Simplifying the system design and fabrication processes and lowering the cost of the devices could bring down the translation barrier for micro/nano-electroporation technologies, potentially promoting the prevalence of advanced healthcare options such as DNA vaccines. While nanotechnology and micro/nano fabrication techniques have largely enhanced the practicality of adopting electroporation *in vivo* for gene therapy, technical hurdles still remain. To fulfill the tissue-level delivery controllability enabled by local administration, implantability is a key consideration for micro/nano-electroporation devices. This entails the wider usage of commercial track-etched nanopore

membranes for NEP devices. These polymeric membranes are a flexible and cost-effective alternative to the rigid silicon-based platforms with custom-fabricated nanochannels.<sup>24,61</sup> However, a worldwide technical concern lies in the degradability of the nanopore membranes. When long-term implantation is required for repeated dosages of gene drugs, micro/nano-electroporation devices show high demand of complete system establishment with biodegradable materials to eliminate the need of a device removal surgery. This scenario potentially accounts for a considerable portion of *in vivo* electroporation-mediated therapies, and therefore the development of a biodegradable material-based nanopore membrane is an issue of high priority to tackle. Theoretically feasible solutions include using femtosecond laser to burn nanopore arrays in ultrathin biodegradable polymeric films, yet the selection of biodegradable polymer and the tuning of femtosecond laser operating parameters is a subject in itself.

In conclusion, advanced micro/nano-electroporation holds tremendous promise in the field of gene therapy, and recent advancements have paved the way for its future applications. With ongoing research and development, addressing challenges, and exploring new directions, micro/nano-electroporation has the potential to revolutionize the field of gene therapy, providing targeted and efficient treatment strategies for various diseases.

## Author contributions

Feng Liu, Rongtai Su, Siqi Wang and Xinran Jiang contributed equally to this work. Feng Liu, Rongtai Su, Siqi Wang and Xinran Jiang contributed to the conceptualization and writing of the original draft. Lingqian Chang and Wei Mu contributed to supervision, funding acquisition, and draft editing.

## Conflicts of interest

There are no conflicts to declare.

## Acknowledgements

This work was supported by the National Key Research and Development Program of China (2023YFC2415900 and 2022YFB3205601), National Natural Science Foundation of China (32071407).

## Notes and references

- 1 T. Athanasopoulos, M. M. Munye and R. J. Yáñez-Muñoz, *Hematol./Oncol. Clin. North Am.*, 2017, **31**, 753–770.
- 2 V. Sudhakar and R. M. Richardson, *Neurotherapeutics*, 2019, **16**, 166–175.
- 3 R. Tang and Z. Xu, *Mol. Cell. Biochem.*, 2020, **474**, 73–81.

- 4 J. R. Mendell, S. Al-Zaidy, R. Shell, W. D. Arnold, L. R. Rodino-Klapac, T. W. Prior, L. Lowes, L. Alfano, K. Berry, K. Church, J. T. Kissel, S. Nagendran, J. L’Italien, D. M. Sproule, C. Wells, J. A. Cardenas, M. D. Heitzer, A. Kaspar, S. Corcoran, L. Braun, S. Likhite, C. Miranda, K. Meyer, K. D. Foust, A. H. M. Burghes and B. K. Kaspar, *N. Engl. J. Med.*, 2017, **377**, 1713–1722.
- 5 S. W. Pipe, F. W. G. Leebeek, M. Recht, N. S. Key, G. Castaman, W. Miesbach, S. Lattimore, K. Peerlinck, P. Van der Valk, M. Coppens, P. Kampmann, K. Meijer, N. O’Connell, K. J. Pasi, D. P. Hart, R. Kazmi, J. Astermark, C. Hermans, R. Klamroth, R. Lemons, N. Visweshwar, A. von Drygalski, G. Young, S. E. Crary, M. Escobar, E. Gomez, R. Kruse-Jarres, D. V. Quon, E. Symington, M. Wang, A. P. Wheeler, R. Gut, Y. P. Liu, R. E. Dolmetsch, D. L. Cooper, Y. Li, B. Goldstein and P. E. Monahan, *N. Engl. J. Med.*, 2023, **388**, 706–718.
- 6 Y. Zong, Y. Lin, T. Wei and Q. Cheng, *Adv. Mater.*, 2023, **35**, e2303261.
- 7 I. K. Herrmann, M. J. A. Wood and G. Fuhrmann, *Nat. Nanotechnol.*, 2021, **16**, 748–759.
- 8 D. A. Savenkova, A. A. Makarova, I. K. Shalik and D. V. Yudkin, *Int. J. Mol. Sci.*, 2022, **23**, 23.
- 9 H. Yin, R. L. Kanasty, A. A. Eltoukhy, A. J. Vegas, J. R. Dorkin and D. G. Anderson, *Nat. Rev. Genet.*, 2014, **15**, 541–555.
- 10 L. Chang, D. Gallego-Perez, C. L. Chiang, P. Bertani, T. Kuang, Y. Sheng, F. Chen, Z. Chen, J. Shi, H. Yang, X. Huang, V. Malkoc, W. Lu and L. J. Lee, *Small*, 2016, **12**, 5971–5980.
- 11 L. M. Mir, *Methods Mol. Biol.*, 2014, **1121**, 3–23.
- 12 Y. Zhang and L. C. Yu, *Curr. Opin. Biotechnol.*, 2008, **19**, 506–510.
- 13 K. Aravindaram and N. S. Yang, *Methods Mol. Biol.*, 2009, **542**, 167–178.
- 14 P. Qin, T. Han, A. C. H. Yu and L. Xu, *J. Controlled Release*, 2018, **272**, 169–181.
- 15 J. Pan, X. Wang, C. L. Chiang, Y. Ma, J. Cheng, P. Bertani, W. Lu and L. J. Lee, *Lab Chip*, 2024, **24**, 819–831.
- 16 C. Lyu, J. Wang, M. Powell-Palm and B. Rubinsky, *Sci. Rep.*, 2018, **8**, 2481.
- 17 Z. Yang, L. Chang, C. L. Chiang and L. J. Lee, *Curr. Pharm. Des.*, 2015, **21**, 6081–6088.
- 18 J. Gehl, *Acta Physiol. Scand.*, 2003, **177**, 437–447.
- 19 Y. Isaka and E. Imai, *Expert Opin. Drug Delivery*, 2007, **4**, 561–571.
- 20 J. Shi, Y. Ma, J. Zhu, Y. Chen, Y. Sun, Y. Yao, Z. Yang and J. Xie, *Molecules*, 2018, **23**, 11.
- 21 L. M. Mir, *Methods Mol. Biol.*, 2008, **423**, 3–17.
- 22 Y. H. Teo, J. H. Yap, H. An, S. C. M. Yu, L. Zhang, J. Chang and K. H. Cheong, *Sensors*, 2022, **22**, 13.
- 23 T. S. Santra, S. Kar, H. Y. Chang and F. G. Tseng, *Lab Chip*, 2020, **20**, 4194–4204.
- 24 L. Chang, L. Li, J. Shi, Y. Sheng, W. Lu, D. Gallego-Perez and L. J. Lee, *Lab Chip*, 2016, **16**, 4047–4062.
- 25 A. Tay and N. Melosh, *Acc. Chem. Res.*, 2019, **52**, 2462–2471.

26 K. Kim and W. G. Lee, *J. Mater. Chem. B*, 2017, **5**, 2726–2738.

27 V. F. Van Tendeloo, P. Ponsaerts and Z. N. Berneman, *Curr. Opin. Mol. Ther.*, 2007, **9**, 423–431.

28 O. Met, E. Balslev, H. Flyger and I. M. Svane, *Breast Cancer Res. Treat.*, 2011, **125**, 395–406.

29 A. Hashemi, F. Roohvand, M. H. Ghahremani, M. R. Aghasadeghi, R. Vahabpour, F. Motevali and A. Memarnejadian, *Cytol. Genet.*, 2012, **46**, 347–353.

30 D. Selmeczi, T. S. Hansen, O. Met, I. M. Svane and N. B. Larsen, *Biomed. Microdevices*, 2011, **13**, 383–392.

31 K. Gao, X. Huang, C. L. Chiang, X. Wang, L. Chang, P. Boukany, G. Marcucci, R. Lee and L. J. Lee, *Mol. Ther.*, 2016, **24**, 956–964.

32 N. Pathak, C. A. Patino, N. Ramani, P. Mukherjee, D. Samanta, S. B. Ebrahimi, C. A. Mirkin and H. D. Espinosa, *Nano Lett.*, 2023, **23**, 3653–3660.

33 A. Alex, V. Piano, S. Polley, M. Stuiver, S. Voss, G. Ciossani, K. Overlack, B. Voss, S. Wohlgemuth, A. Petrovic, Y. Wu, P. Selenko, A. Musacchio and S. Maffini, *eLife*, 2019, **8**, 48287.

34 F. Liu, Z. Yang, R. Yao, H. Li, J. Cheng and M. Guo, *ACS Nano*, 2022, **16**, 19363–19372.

35 K. Kinosita, Jr. and T. Y. Tsong, *Nature*, 1978, **272**, 258–260.

36 H. He, D. C. Chang and Y. K. Lee, *Bioelectrochemistry*, 2007, **70**, 363–368.

37 M. P. Rols and J. Teissié, *Biophys. J.*, 1998, **75**, 1415–1423.

38 U. Zimmermann, G. Pilwat, A. Péqueux and R. Gilles, *J. Membr. Biol.*, 1980, **54**, 103–113.

39 E. P. W. Jenkins, A. Finch, M. Gerigk, I. F. Triantis, C. Watts and G. G. Malliaras, *Adv. Sci.*, 2021, **8**, e2100978.

40 K. Kinosita Jr and T. Y. Tsong, *Nature*, 1977, **268**, 438–441.

41 J. Teissié and M.-P. Rols, *Biophys. J.*, 1993, **65**, 409–413.

42 J. C. Weaver and Y. A. Chizmadzhev, *Bioelectrochem. Bioenerg.*, 1996, **41**, 135–160.

43 T. Kotnik, L. Rems, M. Tarek and D. Miklavčič, *Annu. Rev. Biophys.*, 2019, **48**, 63–91.

44 B. Geboers, H. J. Scheffer, P. M. Graybill, A. H. Ruarus, S. Nieuwenhuizen, R. S. Puijk, P. M. van den Tol, R. V. Davalos, B. Rubinsky, T. D. de Gruijl, D. Miklavčič and M. R. Meijerink, *Radiology*, 2020, **295**, 254–272.

45 J. Pan, C. L. Chiang, X. Wang, P. Bertani, Y. Ma, J. Cheng, V. Talesara, L. J. Lee and W. Lu, *Nanoscale*, 2023, **15**, 4080–4089.

46 M. Khine, A. Lau, C. Ionescu-Zanetti, J. Seo and L. P. Lee, *Lab Chip*, 2005, **5**, 38–43.

47 E. G. Guignet and T. Meyer, *Nat. Methods*, 2008, **5**, 393–395.

48 B. Marrero and R. Heller, *Biomaterials*, 2012, **33**, 3036–3046.

49 M. dal Maschio, D. Ghezzi, G. Bony, A. Alabastri, G. Deidda, M. Brondi, S. S. Sato, R. P. Zaccaria, E. Di Fabrizio, G. M. Ratto and L. Cancedda, *Nat. Commun.*, 2012, **3**, 960.

50 W. Kang, J. P. Giraldo-Vela, S. S. Nathamgari, T. McGuire, R. L. McNaughton, J. A. Kessler and H. D. Espinosa, *Lab Chip*, 2014, **14**, 4486–4495.

51 L. Chang, P. Bertani, D. Gallego-Perez, Z. Yang, F. Chen, C. Chiang, V. Malkoc, T. Kuang, K. Gao, L. J. Lee and W. Lu, *Nanoscale*, 2016, **8**, 243–252.

52 S. Wang and L. J. Lee, *Biomicrofluidics*, 2013, **7**, 11301.

53 L. Schmiderer, A. Subramaniam, K. Žemaitis, A. Bäckström, D. Yudovich, S. Soboleva, R. Galeev, C. N. Prinz, J. Larsson and M. Hjort, *Proc. Natl. Acad. Sci. U. S. A.*, 2020, **117**, 21267–21273.

54 T. Geng, Y. Zhan, J. Wang and C. Lu, *Nat. Protoc.*, 2011, **6**, 1192–1208.

55 T. Geng and C. Lu, *Lab Chip*, 2013, **13**, 3803–3821.

56 B. Duckert, M. Fauvart, P. Goos, T. Stakenborg, L. Lagae and D. Braeken, *J. Controlled Release*, 2022, **352**, 61–73.

57 L. Lin, Y. Wang, M. Cai, X. Jiang, Y. Hu, Z. Dong, D. Yin, Y. Liu, S. Yang and Z. Liu, *Adv. Funct. Mater.*, 2022, **32**, 2109187.

58 J. El-Ali, P. K. Sorger and K. F. Jensen, *Nature*, 2006, **442**, 403–411.

59 X. Hang, Z. Huang, S. He, Z. Wang, Z. Dong and L. Chang, *Small Methods*, 2024, **8**, e2300915.

60 Y. Ma, L. Sun, J. Zhang, C.-l. Chiang, J. Pan, X. Wang, K. J. Kwak, H. Li, R. Zhao and X. Y. Rima, *Adv. Sci.*, 2023, **10**, 2302622.

61 D. Gallego-Pérez, D. Pal, S. Ghatak, V. Malkoc, N. Higuita-Castro, S. Gnyawali, L. Chang, W.-C. Liao, J. Shi and M. Sinha, *Nat. Nanotechnol.*, 2017, **12**, 974–979.

62 W. Kang, F. Yavari, M. Minary-Jolandan, J. P. Giraldo-Vela, A. Safi, R. L. McNaughton, V. Parpoil and H. D. Espinosa, *Nano Lett.*, 2013, **13**, 2448–2457.

63 P. E. Boukany, A. Morss, W. C. Liao, B. Henslee, H. Jung, X. Zhang, B. Yu, X. Wang, Y. Wu, L. Li, K. Gao, X. Hu, X. Zhao, O. Hemminger, W. Lu, G. P. Lafyatis and L. J. Lee, *Nat. Nanotechnol.*, 2011, **6**, 747–754.

64 L. Chang, M. Howdyshell, W. C. Liao, C. L. Chiang, D. Gallego-Perez, Z. Yang, W. Lu, J. C. Byrd, N. Muthusamy, L. J. Lee and R. Sooryakumar, *Small*, 2015, **11**, 1818–1828.

65 Z. Dong, S. Yan, B. Liu, Y. Hao, L. Lin, T. Chang, H. Sun, Y. Wang, H. Li, H. Wu, X. Hang, S. He, J. Hu, X. Xue, N. Wu and L. Chang, *Nano Lett.*, 2021, **21**, 4878–4886.

66 M. Tarek, *Biophys. J.*, 2005, **88**, 4045–4053.

67 O. Met, J. Eriksen and I. M. Svane, *Mol. Biotechnol.*, 2008, **40**, 151–160.

68 C. M. Barbon, L. Baker, C. Lajoie, U. Ramstedt, M. L. Hedley and T. M. Luby, *Vaccine*, 2010, **28**, 7852–7864.

69 A. R. Shokouhi, Y. Chen, H. Z. Yoh, T. Murayama, K. Suu, Y. Morikawa, J. Brenker, T. Alan, N. H. Voelcker and R. Elnathan, *J. Nanobiotechnol.*, 2023, **21**, 273.

70 C. A. Patino, P. Mukherjee, E. J. Berns, E. H. Mouly, L. Stan, M. Mrksich and H. D. Espinosa, *ACS Nano*, 2022, **16**, 7937–7946.

71 J. R. Mendell, S. A. Al-Zaidy, L. R. Rodino-Klapac, K. Goodspeed, S. J. Gray, C. N. Kay, S. L. Boye, S. E. Boye, L. A. George, S. Salabarria, M. Corti, B. J. Byrne and J. P. Tremblay, *Mol. Ther.*, 2021, **29**, 464–488.

72 D. Gallego-Perez, D. Pal, S. Ghatak, V. Malkoc, N. Higuita-Castro, S. Gnyawali, L. Chang, W. C. Liao, J. Shi, M. Sinha, K. Singh, E. Steen, A. Sunyecz, R. Stewart, J. Moore, T. Ziebro, R. G. Northcutt, M. Homsy, P. Bertani, W. Lu, S. Roy, S. Khanna, C. Rink, V. B. Sundaresan, J. J. Otero, L. J. Lee and C. K. Sen, *Nat. Nanotechnol.*, 2017, **12**, 974–979.

73 G. Kougkulos, L. Laudebat, S. Dinculescu, J. Simon, M. Golzio, Z. Valdez-Nava and E. Flahaut, *J. Controlled Release*, 2024, **367**, 235–247.

74 T. Yang, D. Huang, C. Li, D. Zhao, J. Li, M. Zhang, Y. Chen, Q. Wang, Z. Liang, X.-J. Liang, Z. Li and Y. Huang, *Nano Today*, 2021, **36**, 101017.

75 H. Wu, Y. Wang, H. Li, Y. Hu, Y. Liu, X. Jiang, H. Sun, F. Liu, A. Xiao, T. Chang, L. Lin, K. Yang, Z. Wang, Z. Dong, Y. Li, S. Dong, S. Wang, J. Chen, Y. Liu, D. Yin, H. Zhang, M. Liu, S. Kong, Z. Yang, X. Yu, Y. Wang, Y. Fan, L. Wang, C. Yu and L. Chang, *Nat. Electron.*, 2024, **7**, 299–312.

76 G. Schett, A. Mackensen and D. Mougakakos, *Lancet*, 2023, **402**, 2034–2044.

77 T. Inozume, *Exp. Dermatol.*, 2023, **32**, 250–255.

78 P. Sharma and D. M. Kranz, *Crit. Rev. Immunol.*, 2019, **39**, 105–122.

79 S. Ma, X. Li, X. Wang, L. Cheng, Z. Li, C. Zhang, Z. Ye and Q. Qian, *Int. J. Biol. Sci.*, 2019, **15**, 2548–2560.

80 L. Chang, D. Gallego-Perez, X. Zhao, P. Bertani, Z. Yang, C. L. Chiang, V. Malkoc, J. Shi, C. K. Sen, L. Odonnell, J. Yu, W. Lu and L. J. Lee, *Lab Chip*, 2015, **15**, 3147–3153.

81 Y. Liu, K. Adu-Berchie, J. M. Brockman, M. Pezone, D. K. Y. Zhang, J. Zhou, J. W. Pyrdol, H. Wang, K. W. Wucherpfennig and D. J. Mooney, *Proc. Natl. Acad. Sci. U. S. A.*, 2023, **120**, e2213222120.

82 K. Pan, H. Farrukh, V. Chittep, H. Xu, C. X. Pan and Z. Zhu, *J. Exp. Clin. Cancer Res.*, 2022, **41**, 119.

83 K. Si, Z. Dai, Z. Li, Z. Ye, B. Ding, S. Feng, B. Sun, Y. Shen and Z. Xiao, *Cytotherapy*, 2023, **25**, 615–624.

84 J. An, C. P. Zhang, H. Y. Qiu, H. X. Zhang, Q. B. Chen, Y. M. Zhang, X. L. Lei, C. X. Zhang, H. Yin and Y. Zhang, *Nat. Biomed. Eng.*, 2024, **8**, 149–164.

85 M. Breton, L. Delemotte, A. Silve, L. M. Mir and M. Tarek, *J. Am. Chem. Soc.*, 2012, **134**, 13938–13941.

86 Y. K. Oh and T. G. Park, *Adv. Drug Delivery Rev.*, 2009, **61**, 850–862.

87 A. Ptaszniak, Y. Nakata, A. Kalota, S. G. Emerson and A. M. Gewirtz, *Nat. Med.*, 2004, **10**, 1187–1189.

88 D. L. Lewis and J. A. Wolff, *Adv. Drug Delivery Rev.*, 2007, **59**, 115–123.

89 S. N. Campelo, P. H. Huang, C. R. Buie and R. V. Davalos, *Annu. Rev. Biomed. Eng.*, 2023, **25**, 77–100.

90 M. Wang, O. Orwar, J. Olofsson and S. G. Weber, *Anal. Bioanal. Chem.*, 2010, **397**, 3235–3248.

91 P. Kumar, A. Nagarajan and P. D. Uchil, *Cold Spring Harbor Protoc.*, 2019, **2019**, 3.

92 Y. Sheng, Z. Huang, T. Zhang, F. Qian, Y. Zhu, Z. Dong, Q. Zhang, Q. Lei, F. Kong, Y. Wang, M. Walden, S. Wuttke, L. Chang, W. Zhu and J. Hu, *J. Am. Chem. Soc.*, 2022, **144**, 9443–9450.

93 Z. Yang, J. Shi, J. Xie, Y. Wang, J. Sun, T. Liu, Y. Zhao, X. Zhao, X. Wang, Y. Ma, V. Malkoc, C. Chiang, W. Deng, Y. Chen, Y. Fu, K. J. Kwak, Y. Fan, C. Kang, C. Yin, J. Rhee, P. Bertani, J. Otero, W. Lu, K. Yun, A. S. Lee, W. Jiang, L. Teng, B. Y. S. Kim and L. J. Lee, *Nat. Biomed. Eng.*, 2020, **4**, 69–83.

94 L. Lambrecht, A. Lopes, S. Kos, G. Sersa, V. Préat and G. Vandermeulen, *Expert Opin. Drug Delivery*, 2016, **13**, 295–310.

95 T. Kotnik, W. Frey, M. Sack, S. Haberl Meglič, M. Peterka and D. Miklavčič, *Trends Biotechnol.*, 2015, **33**, 480–488.

96 J. C. Park, M. J. Park, S. Y. Lee, D. Kim, K. T. Kim, H. K. Jang and H. J. Cha, *Stem Cell Res. Ther.*, 2023, **14**, 164.

97 R. O. Bak, N. Gomez-Ospina and M. H. Porteus, *Trends Genet.*, 2018, **34**, 600–611.

98 J. Popovitz, R. Sharma, R. Hoshyar, B. Soo Kim, N. Murthy and K. Lee, *Adv. Drug Delivery Rev.*, 2023, **200**, 115026.

99 W. Wen and X. B. Zhang, *Exp. Hematol.*, 2022, **110**, 13–19.

100 F. Memi, A. Ntokou and I. Papangeli, *Semin. Perinatol.*, 2018, **42**, 487–500.

101 W. Qin, S. L. Dion, P. M. Kutny, Y. Zhang, A. W. Cheng, N. L. Jillette, A. Malhotra, A. M. Geurts, Y. G. Chen and H. Wang, *Genetics*, 2015, **200**, 423–430.

102 P. D. Hsu, E. S. Lander and F. Zhang, *Cell*, 2014, **157**, 1262–1278.

103 J. A. Doudna and E. Charpentier, *Science*, 2014, **346**, 1258096.

104 M. Jinek, K. Chylinski, I. Fonfara, M. Hauer, J. A. Doudna and E. Charpentier, *Science*, 2012, **337**, 816–821.

105 T. Wan, J. Zhong, Q. Pan, T. Zhou, Y. Ping and X. Liu, *Sci. Adv.*, 2022, **8**, 9435.

106 S. V. Paffenholz, C. Salvagno, Y. J. Ho, M. Limjoco, T. Baslan, S. Tian, A. Kulick, E. de Stanchina, J. E. Wilkinson, F. M. Barriga, D. Zamarin, J. R. Cubillos-Ruiz, J. Leibold and S. W. Lowe, *Proc. Natl. Acad. Sci. U. S. A.*, 2022, **119**, 5.

107 R. Maresch, S. Mueller, C. Veltkamp, R. Öllinger, M. Friedrich, I. Heid, K. Steiger, J. Weber, T. Engleitner, M. Barenboim, S. Klein, S. Louzada, R. Banerjee, A. Strong, T. Stauber, N. Gross, U. Geumann, S. Lange, M. Ringelhan, I. Varela, K. Unger, F. Yang, R. M. Schmid, G. S. Vassiliou, R. Braren, G. Schneider, M. Heikenwalder, A. Bradley, D. Saur and R. Rad, *Nat. Commun.*, 2016, **7**, 10770.

108 L. Raes, M. Pille, A. Harizaj, G. Goetgeluk, J. Van Hoeck, S. Stremersch, J. C. Fraire, T. Brans, O. G. de Jong, R. Maas-Bakker, E. Mastrobattista, P. Vader, S. C. De Smedt, B. Vandekerckhove, K. Raemdonck and K. Braeckmans, *Mol. Ther. – Nucleic Acids*, 2021, **25**, 696–707.

109 S. Zhang, J. Shen, D. Li and Y. Cheng, *Theranostics*, 2021, **11**, 614–648.

110 F. N. Faruqu, L. Xu and K. T. Al-Jamal, *J. Visualized Exp.*, 2018, **5**, 142.

111 Y. Liang, L. Duan, J. Lu and J. Xia, *Theranostics*, 2021, **11**, 3183–3195.

112 R. Kalluri and V. S. LeBleu, *Science*, 2020, **367**, 6478.

113 S. Dong, X. Liu, Y. Bi, Y. Wang, A. Antony, D. Lee, K. Huntoon, S. Jeong, Y. Ma, X. Li, W. Deng, B. R. Schrank, A. J. Grippin, J. Ha, M. Kang, M. Chang, Y. Zhao, R. Sun, X. Sun, J. Yang, J. Chen, S. K. Tang, L. J. Lee, A. S. Lee, L. Teng, S. Wang, L. Teng, B. Y. S. Kim, Z. Yang and W. Jiang, *Nat. Commun.*, 2023, **14**, 6610.

114 Y. You, Y. Tian, Z. Yang, J. Shi, K. J. Kwak, Y. Tong, A. P. Estania, J. Cao, W. H. Hsu, Y. Liu, C. L. Chiang, B. R. Schrank, K. Huntoon, D. Lee, Z. Li, Y. Zhao, H. Zhang, T. D. Gallup, J. Ha, S. Dong, X. Li, Y. Wang, W. J. Lu, E. Bahrani, L. J. Lee, L. Teng, W. Jiang, F. Lan, B. Y. S. Kim and A. S. Lee, *Nat. Biomed. Eng.*, 2023, **7**, 887–900.

115 M. L. Yarmush, A. Golberg, G. Serša, T. Kotnik and D. Miklavčič, *Annu. Rev. Biomed. Eng.*, 2014, **16**, 295–320.

116 T. Komel, M. Bosnjak, S. Kranjc Brezar, M. De Robertis, M. Mastrodonato, G. Scillitani, G. Pesole, E. Signori, G. Sersa and M. Cemazar, *Bioelectrochemistry*, 2021, **141**, 107843.

117 R. Fusco, G. Perazzolo Gallo, E. Di Bernardo, V. D'Alessio, M. Ronchetti, M. Cadossi and R. Cadossi, *Biomedicines*, 2022, **10**, 8.

118 R. De Bree, B. M. Tijink, C. J. Van Groeningen and C. R. Leemans, *Sarcoma*, 2006, **2006**, 85234.

119 C. Boye, K. Christensen, K. Asadipour, S. DeClemente, M. Francis and A. Bulysheva, *Bioelectrochemistry*, 2022, **144**, 107980.

120 J. M. Escoffre, C. Mauroy, T. Portet, L. Wasungu, C. Rosazza, Y. Gilbart, L. Mallet, E. Bellard, M. Golzio, M. P. Rols and J. Teissié, *Biophys. Rev.*, 2009, **1**, 177.

121 L. Pasquet, S. Chabot, E. Bellard, M. P. Rols, J. Teissié and M. Golzio, *Hum. Gene Ther.: Methods*, 2019, **30**, 17–22.

122 C. Edelblute, C. Mangiameli and R. Heller, *Hum. Gene Ther.*, 2021, **32**, 1360–1369.

123 S. Babiuk, M. E. Baca-Estrada, M. Foldvari, D. M. Middleton, D. Rabussay, G. Widera and L. A. Babiuk, *J. Biotechnol.*, 2004, **110**, 1–10.

124 R. Heller and G. Shi, *Methods Mol. Biol.*, 2021, **2265**, 635–644.

125 T. Komel, M. Omerzel, U. Kamensek, K. Znidar, U. Lamprecht Tratar, S. Kranjc Brezar, K. Dolinar, S. Pirkmajer, G. Sersa and M. Cemazar, *Int. J. Mol. Sci.*, 2023, **24**, 16.

126 M. Savarin, K. Znidar, G. Sersa, T. Komel, M. Cemazar and U. Kamensek, *Int. J. Mol. Sci.*, 2023, **24**, 2755.

127 A. I. Daud, R. C. DeConti, S. Andrews, P. Urbas, A. I. Riker, V. K. Sondak, P. N. Munster, D. M. Sullivan, K. E. Ugen, J. L. Messina and R. Heller, *J. Clin. Oncol.*, 2008, **26**, 5896–5903.

128 J. Cutrera, G. King, P. Jones, K. Kicenuik, E. Gumpel, X. Xia and S. Li, *Curr. Gene Ther.*, 2015, **15**, 44–54.

129 I. Spanggaard, M. Snoj, A. Cavalcanti, C. Bouquet, G. Sersa, C. Robert, M. Cemazar, E. Dam, B. Vasseur, P. Attali, L. M. Mir and J. Gehl, *Hum. Gene Ther.: Clin. Dev.*, 2013, **24**, 99–107.

130 O. Weiland, G. Ahlén, H. Diepolder, M. C. Jung, S. Levander, M. Fons, I. Mathiesen, N. Y. Sardesai, A. Vahlne, L. Frelin and M. Sällberg, *Mol. Ther.*, 2013, **21**, 1796–1805.

131 F. Q. Yang, Y. Y. Yu, G. Q. Wang, J. Chen, J. H. Li, Y. Q. Li, G. R. Rao, G. Y. Mo, X. R. Luo and G. M. Chen, *J. Viral Hepatitis*, 2012, **19**, 581–593.

132 G. J. Wilson, B. Rodriguez, S. S. Li, M. Allen, I. Frank, E. Rudnicki, M. Trahey, S. Kalams, D. Hannaman, D. K. Clarke, R. Xu, M. Egan, J. Eldridge, M. Pensiero, T. Latham, G. Ferrari, D. C. Montefiori, G. D. Tomaras, S. C. De Rosa, J. M. Jacobson, M. D. Miner and M. Elizaga, *Vaccine*, 2023, **41**, 2696–2706.

133 S. C. De Rosa, S. Edupuganti, Y. Huang, X. Han, M. Elizaga, E. Swann, L. Polakowski, S. A. Kalams, M. C. Keefer, J. Maenza, Y. Lu, M. C. Wise, J. Yan, M. P. Morrow, A. S. Khan, J. D. Boyer, L. Humeau, S. White, M. Pensiero, N. Y. Sardesai, M. L. Bagarazzi, D. B. Weiner, G. Ferrari, G. D. Tomaras, D. C. Montefiori, L. Corey and M. J. McElrath, *JCI Insight*, 2020, **5**, 137079.

134 J. M. Jacobson, L. Zheng, C. C. Wilson, P. Tebas, R. M. Matining, M. A. Egan, J. Eldridge, A. L. Landay, D. B. Clifford, A. F. Luetkemeyer, J. Tiu, A. L. Martinez, J. Janik, T. A. Spitz, J. Hural, J. McElrath and N. Frahm, *JAIDS, J. Acquired Immune Defic. Syndr.*, 2016, **71**, 163–171.

135 J. W. Hooper, J. E. Moon, K. M. Paolino, R. Newcomer, D. E. McLain, M. Josley, D. Hannaman and C. Schmaljohn, *Clin. Microbiol. Infect.*, 2014, **20**(Suppl. 5), 110–117.

136 J. Hooper, K. M. Paolino, K. Mills, S. Kvilas, M. Josley, M. Cohen, B. Somerville, M. Wisniewski, S. Norris, B. Hill, M. Sanchez-Lockhart, D. Hannaman and C. S. Schmaljohn, *Vaccines*, 2020, **8**, 377.

137 K. Modjarrad, C. C. Roberts, K. T. Mills, A. R. Castellano, K. Paolino, K. Muthuman, E. L. Reuschel, M. L. Robb, T. Racine, M. D. Oh, C. Lamarre, F. I. Zaidi, J. Boyer, S. B. Kudchodkar, M. Jeong, J. M. Darden, Y. K. Park, P. T. Scott, C. Remigio, A. P. Parikh, M. C. Wise, A. Patel, E. K. Duperret, K. Y. Kim, H. Choi, S. White, M. Bagarazzi, J. M. May, D. Kane, H. Lee, G. Kobinger, N. L. Michael, D. B. Weiner, S. J. Thomas and J. N. Maslow, *Lancet Infect. Dis.*, 2019, **19**, 1013–1022.

138 F. Eriksson, T. Tötterman, A. K. Maltais, P. Pisa and J. Yachnin, *Vaccine*, 2013, **31**, 3843–3848.

139 M. L. Bagarazzi, J. Yan, M. P. Morrow, X. Shen, R. L. Parker, J. C. Lee, M. Giffear, P. Pankhong, A. S. Khan, K. E. Broderick, C. Knott, F. Lin, J. D. Boyer, R. Draghia-Akli, C. J. White, J. J. Kim, D. B. Weiner and N. Y. Sardesai, *Sci. Transl. Med.*, 2012, **4**, 155.

140 C. L. Trimble, M. P. Morrow, K. A. Kraynyak, X. Shen, M. Dallas, J. Yan, L. Edwards, R. L. Parker, L. Denny, M. Giffear, A. S. Brown, K. Marcozzi-Pierce, D. Shah, A. M. Slager, A. J. Sylvester, A. Khan, K. E. Broderick, R. J. Juba, T. A. Herring, J. Boyer, J. Lee, N. Y. Sardesai, D. B. Weiner and M. L. Bagarazzi, *Lancet*, 2015, **386**, 2078–2088.

141 T. J. Kim, H. T. Jin, S. Y. Hur, H. G. Yang, Y. B. Seo, S. R. Hong, C. W. Lee, S. Kim, J. W. Woo, K. S. Park, Y. Y. Hwang, J. Park, I. H. Lee, K. T. Lim, K. H. Lee, M. S. Jeong, C. D. Surh, Y. S. Suh, J. S. Park and Y. C. Sung, *Nat. Commun.*, 2014, **5**, 5317.

142 J. Yuan, G. Y. Ku, M. Adamow, Z. Mu, S. Tandon, D. Hannaman, P. Chapman, G. Schwartz, R. Carvajal, K. S. Panageas, A. N. Houghton and J. D. Wolchok, *J. Immunother. Cancer*, 2013, **1**, 20.

143 A. Muralidharan and P. E. Boukany, *Trends Biotechnol.*, 2023, **23**, 331.